NTNU
Norwegian University of
Science and Technology

Analyzing the Integration of Renewable Energy in Interconnected Power Systems Using a Flow-based Market Model

Arne Øvrebø Lie
Eirik Andre Rye

Master of Energy and Environmental Engineering
Submission date: June 2016
Supervisor: Hossein Farahmand, ELKRAFT
Co-supervisor: Magnus Korpås, ELKRAFT
Harald G. Svendsen, SINTEF Energy Research

Norwegian University of Science and Technology
Department of Electric Power Engineering

Abstract

As renewable energy is taking on a more pivotal role in power systems around the world, the implications of this development are all the more significant. The study of these issues requires accurate models with publicly available data, so that peer-reviewed analyses rooted in realistic preconditions may be performed.

This thesis addresses some of these issues in three studies using the PowerGAMA simulation tool. First, an existing PowerGAMA model is expanded, updated and validated to include most of the 2014 ENTSO-E power system. Comparison of the simulation results with actual data on cross-border flows and energy mix for 2014 shows acceptable correlation, and the model is able to reproduce the main characteristics of the power system, like reservoir handling, hydro pump behavior and seasonal variations in cross-border flows. Two case studies are performed to illustrate the model's application and limitations when studying large-scale integration of renewable energy.

The first case study investigates a 2030 scenario for the Moroccan power system with increased renewable generation capacity and demand in order to identify challenges that need to be addressed. Particular emphasis is put on a cost-benefit analysis comparing investments in storage capabilities for concentrated solar power and grid reinforcements. Our results indicate that large investments in electric infrastructure is needed to accommodate the renewable commitment and demand increase. Furthermore, 16 branch investments can be the preferable investment strategy for Morocco, with an annual cost reduction of 279 M€.

The second case study investigates how different renewable technologies affect the utilization of existing pumped hydro plants in the Spanish power system. The approach is able to reproduce the actual hydro characteristics and ensures reasonable reservoir handling. Three scenarios are investigated, all doubling the current renewable energy output. Our results indicate that an increase in renewable generation increases the utilization of pumped hydro storage. For the scenarios with added wind and solar, and only added wind, the utilization is increased by around 150 %. The largest increase is observed in the solar scenario, at 189 %, due to a larger price reduction during solar hours.

In conclusion, the PowerGAMA model gives a reasonable picture of reality and is suited for future analysis, to which some suggestions are presented.

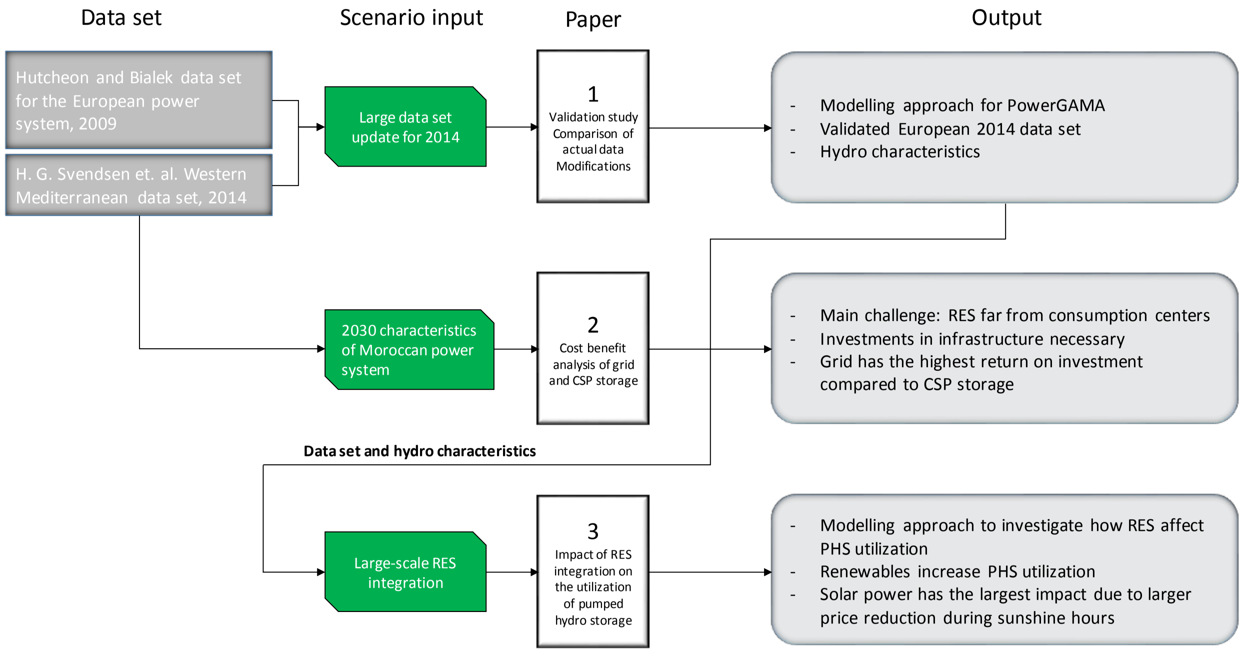
Data set
Scenario input
Paper
Output
Hutcheon and Bialek data set for the European power system, 2009
H. G. Svendsen et. al. Western Mediterranean data set, 2014
Large data set update for 2014
1
Validation study
Comparison of actual data
Modifications
- Modelling approach for PowerGAMA
- Validated European 2014 data set
- Hydro characteristics
2030 characteristics of Moroccan power system
2
Cost benefit analysis of grid and CSP storage
- Main challenge: RES far from consumption centers
- Investments in infrastructure necessary
- Grid has the highest return on investment compared to CSP storage
Data set and hydro characteristics
Large-scale RES integration
3
Impact of RES integration on the utilization of pumped hydro storage
- Modelling approach to investigate how RES affect PHS utilization
- Renewables increase PHS utilization
- Solar power has the largest impact due to larger price reduction during sunshine hours

Figure 0.1: Flowchart showing the organization of the thesis

Sammendrag

Ettersom fornybar energi spiller en stadig viktigere rolle i kraftsystemer verden over, blir virkningene av denne utviklingen desto mer betydningsfulle. For å studere problemstillinger knyttet til dette kreves nøyaktige modeller med offentlig tilgjengelige data, slik at fagfellevurderte analyser bygget på realistiske antagelser kan utføres.

Denne oppgaven tar opp noen av disse problemstillingene ved hjelp av simuleringsverktøyet PowerGAMA. Først utvides, oppdateres og valideres en eksisterende modell for PowerGAMA, slik at den omfavner det meste av ENTSO-E-kraftsystemet i 2014. Sammenligninger av resultatene fra simuleringen med faktiske data for energimiks og kraftflyt mellom land viser akseptabel korrelasjon, og modellen er i stand til å gjenskape hovedegenskapene til kraftsystemet, slik som reservoarhåndtering, pumpekraft og sesongvariasjoner i kraftflyt mellom land. Videre blir det gjennomført to case-studier for å vise modellens anvendelsesområde og begrensninger ved studier av innføring av fornybar energi i stor skala.

I den første case-studien studeres et 2030-scenario for det marokkanske kraftsystemet med økt fornybar energi og etterspørsel, slik at potensielle utfordringer kan undersøkes. Spesiell vekt er lagt på en kost-nytte-analyse som sammenligner energilager med forsterking av nettet. Resultatene indikerer at store investeringer i kraftinfrastruktur er nødvendige for å håndtere fornybarforpliktelsen og den økte etterspørselen. Videre kan 16 linjeinvesteringer være den foretrukne investeringsstrategien for Marokko, med årlige kostnadsbesparelser på 279 M€.

Den andre case-studien undersøker hvordan forskjellige fornybarteknologier påvirker bruken av pumpekraft i det spanske kraftsystemet. Tilnærmingen gjenskaper de faktiske vannkraftkarakteristikkene og sikrer fornuftig reservoarhåndtering. Tre forskjellige scenarier blir undersøkt, og i alle blir den nåværende produksjonen av fornybar energi doblet. Resultatene indikerer at en økning i fornybarproduksjon øker bruken av pumpekraft. I scenariene med både økt vind og sol, og bare vind, er økningen rundt 150%. Den største økningen sees i solscenariet med 189%, ettersom prisfallet er større i løpet av soltimene.

Avslutningsvis gir PowerGAMA-modellen et rimelig bilde av virkeligheten. Den er egnet for videre analyser, og forslag til disse blir presentert i konklusjonen.

Preface

This master's thesis was written at the Department of Electric Power Engineering at the Norwegian University of Science and Technology (NTNU) during the spring semester 2016.

With the combined support from all three supervisors we reached our goal of writing three scientific papers. A special thanks goes to Prof. Hossein Farahmand, our responsible professor, who both trusted us to work independently choosing our own approach, and gave us great guidance in our work when needed. Dr. Harald Svendsen at SINTEF Energy, one of the creators of PowerGAMA, for indispensable help at both teaching us the functionality of the tool, as well as helping us further develop the scripts we needed to support our analyses. Last, but not least, Prof. Magnus Korpås, for great work supervising our project and master's thesis, and the idea of focusing on writing scientific papers, a great format which enabled us to both learn about, and contribute to, scientific work. As a result, one paper was accepted for presentation at the *European Energy Markets 2016* conference and will be published in IEEExplore, while the other two are submitted for reviews at the time of writing.

Contents

Abbreviations **viii**

List of Figures **xi**

1 Introduction **1**
- 1.1 Scope . . . 2
- 1.2 Organization of this thesis . . . 3

2 Theory **5**
- 2.1 Nodal Pricing . . . 5
- 2.2 DC Power Flow Method . . . 6
- 2.3 Optimization . . . 11
- 2.4 Return on investment . . . 13
- 2.5 Functions for renewable share . . . 14

3 Method **15**
- 3.1 PowerGAMA . . . 15
  - 3.1.1 Input data structure . . . 18
  - 3.1.2 Model input data . . . 18
  - 3.1.3 Modelling of energy storage . . . 19
  - 3.1.4 Modelling of pumped hydro storage . . . 21
  - 3.1.5 Scripts . . . 21
  - 3.1.6 Important cost functions in PowerGAMA . . . 21

4 Conclusion and Further Work **25**
- 4.1 Conclusion . . . 25
- 4.2 Further Work . . . 26

Bibliography **29**

Appendices

A Paper I **31**

B Paper II **43**

C Paper III **51**

D Scripts **61**

Abbreviations

CSP	Concentrated Solar Power
EMPS	EFI's Multi-area Power-market Simulator
GDP	Gross Domestic Product
IEA	International Energy Agency
LP	Linear Programming
MASEN	Moroccan Agency for Solar Energy
OPF	Optimal Power Flow
RE	Renewable Energy
RES	Renewable Energy Source
ROI	Return on investment
TSO	Transmission System Operator
PowerGAMA	Power Grid and Market Analysis tool
PSST	Power System Simulation Tool
PHS	Pumped Hydro Storage
PV	Photovoltaic

List of Figures

0.1 Flowchart showing the organization of the thesis ii

2.1 Three-node example grid 8

3.1 Location of nodes and branches in PowerGAMA 15
3.2 PowerGAMA flowchart [12] 16
3.3 Storage value and correction factor for thermal storage 20
3.4 Generator with storage and pumping [10] 21

D.1 Plot of weekly hydro characteristics for Spain. 68
D.2 Plot of pump percentiles per hour for Spain. 70

1 | Introduction

The power system as we know it is changing at a faster pace than ever. Intermittent renewable energy, higher inter-connectivity, smart grid technologies, distributed generation, consumer flexibility and more storage capabilities are just some of the drivers for the future power system. The changes are largely a consequence of ambitious renewable energy targets, backed by subsidies, laws and regulations. The IEA World Energy Outlook 2015 reports the following: *"Renewables contributed almost half of the world's new power generation capacity in 2014. The coverage of mandatory energy efficiency regulation worldwide expanded to more than a quarter of global consumption."* [1]. Although this is good news for the environment, it further complicates power systems planning and operation. As renewable energy plants are built in locations where the energy resources are good, often away from load centers, the power flow patterns are altered, likely leading to grid congestion. Further, technologies like wind, solar and run-of-river power plants have limited predictability and controllability, complicating generation and load balancing.

The transition towards more renewable energy requires many long-term investments, both in renewable generation facilities, balancing services, as well as infrastructure to enable the new power flow from these facilities to reach consumption centers. Due to the large costs associated with infrastructure investments, long planning and construction times, and long life times, it is crucial to identify the location of future power plants and potential grid bottlenecks at an early stage. How the different technologies interact with each other and affect the power system also becomes a crucial insight, as it affects both the profitability of these projects and power systems operation.

For researchers, good models with publicly available data are of key importance to study these issues. Since the current European power grid is one of the largest interconnected power systems in the world, it is sensible to simulate the whole system for multiple reasons. By utilizing a large data set, some of the complications related to modeling the variability of renewable energy sources are diminished due to cross-border flows, as peak inflow and demand varies for each country. This gives a more realistic analysis when simulating scenarios for large-scale integration of renewable energy. Additionally, the model can be used as a basis to analyze the effect of other major shifts in the energy sector, like the impact of large power plant investments or shut downs, e.g. the nuclear phase-out in Germany, new interconnections, or future case studies of large-scale integration of renewable energy.

Hutcheon and Bialek[1] have put in substantial work to develop an approximate model that includes most of the European transmission system for 2009. Due to the rapid changes in generation mix with increased renewable penetration over the past few years, this model is already loosing some of its applicability. The large EU-projects EuroSunMed[2] and Twenties[3] have developed models and performed analyses of future scenarios for the European power markets with a high penetration of wind and solar power. In association with these projects, SINTEF Energy Research has developed a model for the Western Mediterranean region in 2014. However, a complete model of the European transmission system is not yet established.

1.1 Scope

The main objective of this master's thesis is to establish an updated model of the European power system, which is suitable for analyses of the aforementioned changes, especially the large-scale integration of renewable energy. The model is built specifically for PowerGAMA, a DC optimal power flow-based simulation tool. The data used to build and validate the model is required to be publicly available, putting certain limitations on the level of detail, most notably the marginal cost of individual generators.

Attention is also given to the necessary adjustments of the model to ensure its validity, emphasizing seasonal variations. It should be noted that the model is only compared to actual data from the year 2014, and is not evaluated against other years.

To illustrate the model's application, two case studies are performed. The first is a cost-benefit analysis of concentrated solar power storage and grid investments in a future scenario for the Moroccan power system with a high penetration of renewable energy. The second is an analysis of the implications of renewable energy expansion for pumped hydro storage in Spain. Both are based on the established model, and the acquisition of additional data is adherent to the same principles as the 2014 model. In both case studies the approach is thoroughly discussed to highlight the possibilities and limitations of the model and the simulation tool.

---

[1] http://www.powerworld.com/bialek

[2] http://www.eurosunmed.eu/

[3] http://www.twenties-project.eu/node/1

1.2 Organization of this thesis

This thesis is presented as a collection of three scientific papers listed below and provided in the appendix:

- **A. Validation study of an approximate 2014 European power-flow model using PowerGAMA**
- **B. Analyzing large-scale renewable energy integration and energy storage in Morocco using a flow-based market model**
- **C. The impact of large-scale renewable energy integration on the utilization of pumped hydro storage in Spain**

The remainder of the thesis is organized as follows:

Chapter 2 presents relevant theory to enable the reader to understand how the PowerGAMA simulation tool works.
Chapter 3 briefly explains PowerGAMA, how it differs from similar tools, and its development for this thesis.
Chapter 4 draws the main conclusions and suggests further work.

2 | Theory

To enable the reader to understand how the PowerGAMA simulation tool works, theory of nodal pricing, power flow equations and the optimization algorithm is presented. Additionally, functions for renewable share and theory about return on investment are presented, as these are utilized in the papers.

2.1 Nodal Pricing

Nodal pricing, also known as locational marginal pricing (LMP), is a method for determining prices in wholesale electricity markets for a number of locations in the grid, called nodes. Each node represent a physical location in the transmission system where energy is withdrawn by loads, and/or injected by generators. The calculation of prices reflect the value of electric energy at different geographical locations, accounting for the generation, demand and physical limitation of the transmission system. In other words, the nodal price is the marginal cost of supplying electricity to the node. The nodal price is often refereed to as the shadow price, as it is the dual value of the load balance constraint from the optimization problem.

$$Nodal\ Price = Marginal\ Cost\ of\ \ (Generation + Losses + Congestion) \tag{2.1}$$

If a system does not have any constraints or losses, all nodal prices would be equal, only reflecting the cost of the next unit increment of load in a node. In this case, the generator with the lowest cost would serve the incremental unit, and energy from that generator would be able to flow unconstrained and without losses to any node in the network. In reality, this is not the case, as losses are always present, and congestion can prevent lower cost generators from serving the load. Even in the absence of congestion the nodal pries varies in the different nodes, because of the marginal cost of the physical losses of transporting energy [2]. In other words, with nodal pricing the associated costs are allocated to each node in a manner that recognizes their individual contribution to the extra cost.

Losses occur due to the physical characteristics (impedance) of the power system. The impedance signifies the opposition of power flow, and a higher impedance indicates more opposition to the flow, and thus higher losses. The impedance between two nodes is related to the branch length, number of parallel paths, voltage level, transformers and other electrical equipments between the two nodes. A constraint is caused when a branch reaches its thermal limit, or when it reaches its security limit. As power will flow all available paths to get from the supply point to the consumption, and transmission lines do not control or limit the amount of power they transfer, security limits are managed by the TSO by dispatching the system [3].

In most real systems the algorithm employed is a DC power flow model rather than an AC power flow model, so constraints and re-dispatch resulting from thermal or security limits are identified, but constraints and re-dispatch resulting from reactive power deficiencies are not. This is also the case for PowerGAMA, which uses DC power flow equation as explained in Chapter 2.2. The PowerGAMA model is designed without losses and security limits, meaning only congestion is taken into account. The nodal-prices in PowerGAMA are determined by the algorithm described above, balancing supply and demand in each node from all available generator units. The process is carried out for each time-step, which can manually be set in PowerGAMA. In this analysis, hourly time-steps are used.

Nodal pricing is not a widespread market design, but is used in New Zealand and some American States (Pennsylvania, New Jersey and Maryland), as well as a variation of nodal pricing in Australia. In the Nordic countries zonal pricing is used, which is comparable to nodal pricing, but on an aggregated level. There are both benefits and disadvantages [4] with this market design, and further reading for those interested is advised.

2.2 DC Power Flow Method

In steady state the net active and reactive power entering the AC network at node i is described by the following non-linear equations [5]:

$$P_i = V_i \sum_{j=1}^{n} V_j (G_{ij} \cos(\delta_i - \delta_j) + B_{ij} \sin(\delta_i - \delta_j)) \tag{2.2}$$

$$Q_i = V_i \sum_{j=1}^{n} V_j (G_{ij} \sin(\delta_i - \delta_j) - B_{ij} \cos(\delta_i - \delta_j)) \tag{2.3}$$

where
P_i : Active power balance, node i [MW]
Q_i : Reactive power balance, node i [MVar]
i, j : Node indices
n : Number of nodes
V_i : Voltage magnitude, node i [V]
δ_i : Voltage angle, node i [°]
δ_j : Voltage angle, node j [°]
G_{ij} : Conductance between node i and j with negative sign [S]
G_{ii} : Sum of all conductances connected to node i [S]
B_{ij} : Susceptance between node i and j with negative sign [S]
B_{ii} : Sum of all susceptances connected to node i [S]

Thus, the power flow balance of each node is governed by the branch flows and shunts connected to the respective node. Equations 2.2 and 2.3 may be utilized to determine the magnitude and angle of the voltages at all nodes, or to determine the power flows, losses and currents if the voltages are known.

Equations 2.2 and 2.3 are linearized through certain approximations, known as the DC power flow method, in order to solve the system optimization problem in PowerGAMA. This gives a good approximation of the active power flow in the transmission network [6]. The method is illustrated through an example grid with three interconnected nodes (node and line parameters explained in Figure 2.1) to simplify the notations.

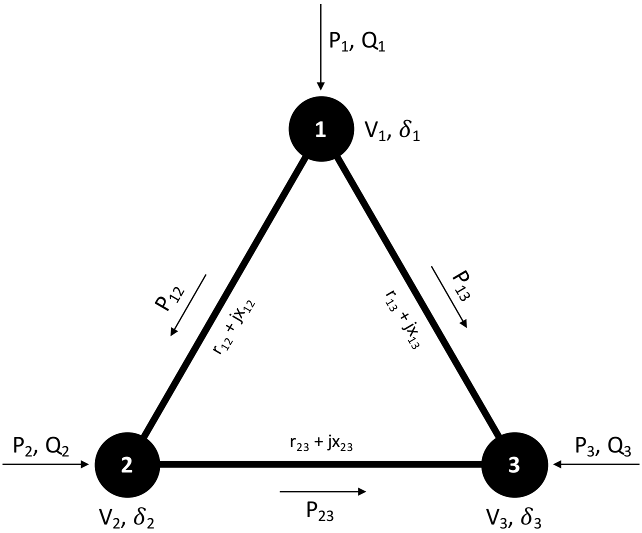
P1, Q1
1
V1, δ1
P12
r12 + jx12
P13
r13 + jx13
P2, Q2
2
r23 + jx23
3
P3, Q3
P23
V2, δ2
V3, δ3

Figure 2.1: Three-node example grid

The complex admittance (Y) consists of a real part, conductance (G), and an imaginary part, susceptance (B), given by:

$$Y = G + jB = \frac{r}{r^2 + x^2} + j\frac{-x}{r^2 + x^2} \tag{2.4}$$

where r is the resistance and x the reactance, both measured in ohms. Normally, the resistance in the grid is significantly lower than the reactance. Inn accordance with Equation 2.4, the conductance and the susceptance can then be approximated as

$$r << x \rightarrow G \approx 0 \quad \text{and} \quad B \approx \frac{-1}{x} \tag{2.5}$$

Equations 2.2 and 2.3 are now given as

$$P_i = V_i \sum_{j=1}^{n} V_j (B_{ij} \sin(\delta_i - \delta_j)) \tag{2.6}$$

$$Q_i = V_i \sum_{j=1}^{n} V_j (-B_{ij} \cos(\delta_i - \delta_j)) \tag{2.7}$$

Further, the voltage angle between two buses is normally small when the power system is operated at steady state. The sine and cosine of the voltage angle may then be approximated as

$$\sin\delta \approx \delta \quad \text{and} \quad \cos\delta \approx 1 \tag{2.8}$$

Equations 2.6 and 2.7 are now given as

$$P_i = V_i \sum_{j=1}^{n} V_j (B_{ij}(\delta_i - \delta_j)) \tag{2.9}$$

$$Q_i = V_i \sum_{j=1}^{n} V_j (-B_{ij}) \tag{2.10}$$

Utilizing the per unit system[1] and assuming that the magnitude of the voltages are about equal to the reference voltage, we get the following approximation:

$$V_i, V_j \approx 1 \tag{2.11}$$

Equations 2.9 and 2.10 are now given as

$$P_i = \sum_{j=1}^{n} B_{ij}(\delta_i - \delta_j) \tag{2.12}$$

$$Q_i = \sum_{j=1}^{n} -B_{ij} \tag{2.13}$$

As seen from Equation 2.13, Q_i is now a constant term, thus it does not impact the flow in the system. Subsequently, the voltage angles for a certain generation and load can be found using only the active power P_i, given by Equation 2.12. Applying this equation to the three node example yields:

$$\mathbf{P} = \begin{bmatrix} P_1 \\ P_2 \\ P_3 \end{bmatrix} = \begin{bmatrix} B_{12}+B_{13} & -B_{12} & -B_{13} \\ -B_{21} & B_{21}+B_{23} & -B_{23} \\ -B_{31} & -B_{32} & B_{31}+B_{32} \end{bmatrix} \times \begin{bmatrix} \delta_1 \\ \delta_2 \\ \delta_3 \end{bmatrix} = \mathbf{B'} \times \boldsymbol{\delta} \tag{2.14}$$

---

[1] In the per unit system the voltage of the reference node is normalised to 1.

where $B'_{ij} = B'_{ji}$ when $i \neq j$, corresponding to the negative value of the susceptance of the line between nodes i and j, thus the matrix is symmetric. In the main diagonal, B'_{ii} is the sum of the susceptances of the lines connected to node i.

From Equation 2.14 the voltage angles are given as:

$$\boldsymbol{\delta} = \begin{bmatrix} \delta_1 \\ \delta_2 \\ \delta_3 \end{bmatrix} = \begin{bmatrix} B_{12} + B_{13} & -B_{12} & -B_{13} \\ -B_{21} & B_{21} + B_{23} & -B_{23} \\ -B_{31} & -B_{32} & B_{31} + B_{32} \end{bmatrix}^{-1} \times \begin{bmatrix} P_1 \\ P_2 \\ P_3 \end{bmatrix} = \mathbf{B'}^{-1} \times \mathbf{P} \tag{2.15}$$

The injected power P_i in Equation 2.15 is not dependent on the absolute value of the voltage angles δ_i, but only on the differences between them. As we can obtain one of the equations by combining the other two, we are left with a singular matrix, i. e. its determinant is zero. These equations are dependent, and there are infinitely many solutions. A unique solution is found by creating a reference point for the system's absolute angle values, so that one of the main diagonal entries have an extra value. The reference point, or the reference bus angle, is set to zero. Setting node 1 as the reference bus in our example, meaning $\delta_1 = 0$, reduces the $\mathbf{B'}$ matrix. The associated column and row, the first of both, are eliminated, making it possible to compute the remaining angles:

$$\begin{bmatrix} \delta_2 \\ \delta_3 \end{bmatrix} = \begin{bmatrix} B_{21} + B_{23} & -B_{23} \\ -B_{32} & B_{31} + B_{32} \end{bmatrix}^{-1} \times \begin{bmatrix} P_2 \\ P_3 \end{bmatrix} \tag{2.16}$$

So far we have found found a way to calculate the voltage angles, but not the branch flows. Looking at one term from the summation in Equation 2.12, we see that the flow on a branch from node i to node j may be written:

$$P_{ij} = B_{ij}(\delta_i - \delta_j) \tag{2.17}$$

On a general form, where the branch from node i to node j is denoted as branch k, the active power flow on the branch may be computed using the angles from 2.16 and the following equation:

$$\mathbf{P_B} = (\mathbf{D} \times \mathbf{A}) \times \boldsymbol{\delta} \tag{2.18}$$

where
P_{Bk} = Power flow, branch k
D_{kk} = The susceptance of branch k with negative sign,
all other elements in $\mathbf{D}$ are zero
k = Branch index
A = The node-arc incidence matrix

In the node-arc incidence matrix, element A_{kj} is 1 if branch k begins at node j, -1 if branch k ends at node j, and 0 otherwise. Applying Equation 2.18 to our three node example yields:

$$\mathbf{P_B} = \begin{bmatrix} P_{B1} \\ P_{B2} \\ P_{B3} \end{bmatrix} = \left(\begin{bmatrix} B_{12} & 0 & 0 \\ 0 & B_{13} & 0 \\ 0 & 0 & B_{23} \end{bmatrix} \times \begin{bmatrix} 1 & -1 & 0 \\ 1 & 0 & -1 \\ 0 & 1 & -1 \end{bmatrix} \right) \times \begin{bmatrix} \delta_1 \\ \delta_2 \\ \delta_3 \end{bmatrix} \tag{2.19}$$

$$\mathbf{P_B} = \begin{bmatrix} P_{B1} \\ P_{B2} \\ P_{B3} \end{bmatrix} = \begin{bmatrix} B_{12}(\delta_1 - \delta_2) \\ B_{13}(\delta_1 - \delta_3) \\ B_{23}(\delta_2 - \delta_3) \end{bmatrix} \tag{2.20}$$

Note that the order of the branches k may be chosen arbitrarily, as long as the order is consistent in $\mathbf{P_B}$, $\mathbf{D}$ and $\mathbf{A}$.

2.3 Optimization

From Section 2.2 we have obtained the linearized power flow equations through the DC power flow method, which make it possible to minimize the system cost using linear programming (LP) for each time-step. The sequential approach in PowerGAMA implies a highly flexible energy market which might be too optimistic, on the other hand future power markets should aim to have a very high degree of flexibility to accommodate a high share of renewable energy.

An advantage of a linear objective function is the short computational time, and that convergence is ensured. Fewer input parameters are also required, as can be seen below. The linear optimization problem has the following sets, indices, parameters and variables for each time-step:

Sets

$\mathcal{G}$: Set of generators

$\mathcal{S}$: Set of pumps

$\mathcal{F}$: Set of flexible loads

$\mathcal{N}$: Set of nodes

$\mathcal{K}$: Set of AC and DC branches

Indices

g : Generator

s : Pump

f : Flexible load

n : Node

k : Branch

Parameters

C_g^{gen} : Cost, generator g [€/MWh]

C_s^{pump} : Cost, pump s [€/MWh]

C_f^{flex} : Cost, flexible load f [€/MWh]

C^{shed} : Fixed cost of load shedding [€/MWh]

P_k^{max} : Branch capacity, branch k [MW]

P_g^{min} : Minimum production, generator g [MW]

P_g^{limit} : Available power[2] generator g [MW]

$P_s^{pump,max}$: Pump capacity, pump s [MW]

$P_f^{flex,max}$: Maximum demand at flexible load f [MW]

P_n^{cons} : Consumption at node n [MW]

Variables

p_g^{gen} : Generation by generator g [MW]

p_s^{pump} : Pump power demand, pump s [MW]

p_f^{flex} : Flexible load f [MW]

p_n^{shed} : Load shedding, node n [MW]

δ_n : Power angle, node n [°]

$p_k^{ac/dc}$: Power flow, AC/DC branch k [MW]

---

[2] Non-storage generators: equal to inflow, with storage: the minimum of generation capacity and inflow plus stored energy.

When SC denotes the system cost of the entire system, the objective function is:

$$\min SC = \sum_{g\in\mathcal{G}} C_g^{gen} p_g^{gen} - \sum_{s\in\mathcal{S}} C_s^{pump} p_s^{pump} - \sum_{f\in\mathcal{F}} C_f^{flex} p_f^{flex} + \sum_{n\in\mathcal{N}} C^{shed} p_n^{shed} \tag{2.21}$$

subject to:

$$-P_k^{max} \leq p_k \leq P_k^{max}, \quad k \in \mathcal{K} \tag{2.22}$$

$$P_g^{min} \leq p_g^{gen} \leq P_g^{limit}, \quad g \in \mathcal{G} \tag{2.23}$$

$$0 \leq p_s^{pump} \leq P_s^{pump,max}, \quad s \in \mathcal{S} \tag{2.24}$$

$$0 \leq p_f^{flex} \leq P_f^{flex,max}, \quad f \in \mathcal{F} \tag{2.25}$$

where 2.22-2.25 are the constraints which delimit the variables. From Section 2.2 we have the power flow constraints 2.26 and 2.28:

$$\mathbf{P} = \mathbf{B'} \times \boldsymbol{\delta} \tag{2.26}$$

where P_n is the power injection at each node, given by:

$$P_n = \sum_{g\in\mathcal{G}_n} p_g^{gen} - \sum_{s\in\mathcal{S}_n} p_s^{pump} - P_n^{cons} + p_n^{shed} + \sum_{k\in\mathcal{K}_n^{dc}} p_k^{dc} \tag{2.27}$$

and

$$\mathbf{P_B} = (\mathbf{D} \times \mathbf{A}) \times \boldsymbol{\delta} \tag{2.28}$$

which describes the flow on the AC branches only. The last constraint is:

$$\delta_1 = 0 \tag{2.29}$$

which was also explained in Section 2.2.

2.4 Return on investment

Return on investment (ROI), given as a percentage, evaluates the efficiency of an investment, and can be used to compare different types of investment scenarios [7]. To calculate the return on investment, the cost of the investment is subtracted from the gain of the investment, and divided by the cost of the investment, as illustrated in equation 2.30.

$$\text{ROI} = \frac{\text{Gain from investment} - \text{Cost of investment}}{\text{Cost of investment}} \tag{2.30}$$

If the result is positive, the investment is profitable, and if its negative, it is unprofitable. For example, if a project has a 100% ROI, the gain from a project is double the investment cost. Gains and costs are not precisely defined, but should include all expected costs, returns, the time value of money, and in some cases also risk and uncertainties.

2.5 Functions for renewable share

There are multiple ways to define the renewable share of a system. The most frequently used is installed renewable capacity divided by total installed capacity.

$$Renewable\ capacity\ share\ = \frac{\sum_{g \in \mathcal{R}} P_g^{cap}}{\sum_{g \in \mathcal{G}} P_g^{cap}} \tag{2.31}$$

where
$\mathcal{R}$: Set of renewable energy generators
P_g^{cap} : Installed capacity of generator g [MW]

Another frequently used parameter is renewable energy share, the sum of renewable energy production (MWh) divided by total consumption (MWh). This is often used as renewable energy sources have a low capacity utilization time compared to conventional power plants, and the actual energy output over time will normally not equal the installed capacity.

$$Renewable\ energy\ share = \frac{\sum_{g \in \mathcal{R}} p_g^{gen}}{\sum_{g \in \mathcal{G}} p_g^{gen}} \tag{2.32}$$

where p_g^{gen} is the generator output over the time period.

3 | Method

The research work is conducted using PowerGAMA (Power Grid and Market Analysis), a flow-based market simulator. The functionality of the tool, the input data and structure, as well as developed scripts are presented in this chapter.

3.1 PowerGAMA

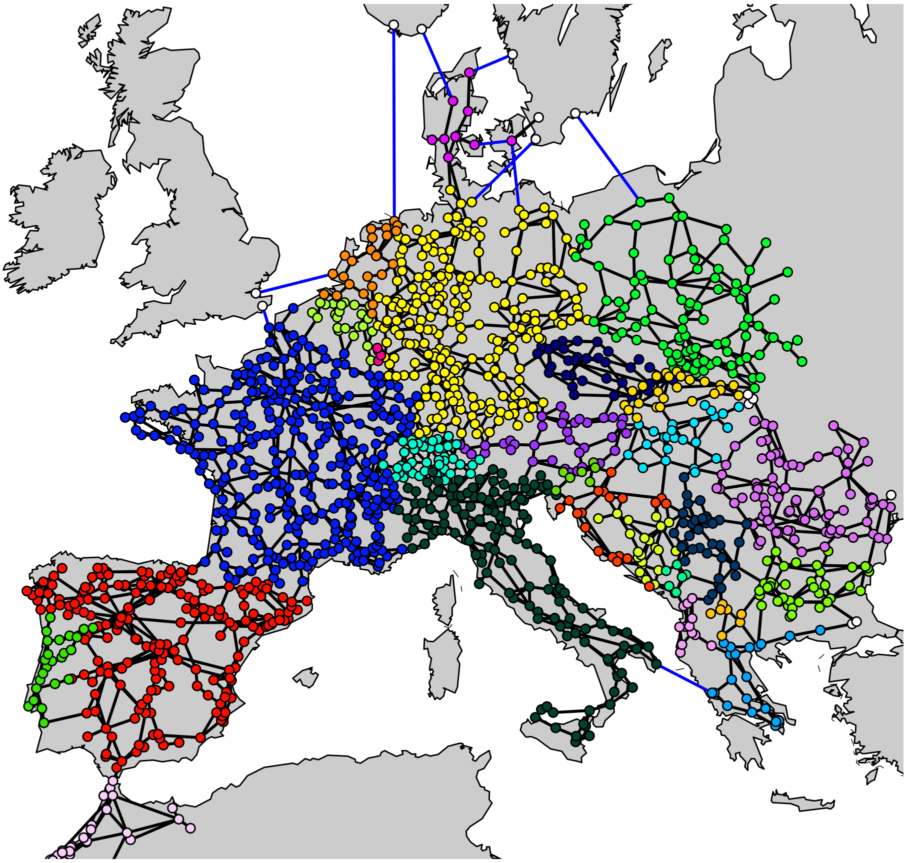

Figure 3.1: Location of nodes and branches in PowerGAMA

PowerGAMA originates from SINTEF's Matlab-based Power System Simulation Tool (PSST) [8], [9], but is written from scratch as an open-source Python model by SINTEF Energy Research for the EU project EuroSunMed. PowerGAMA is a lightweight simulation tool for high level analysis of large interconnected power systems [10]. The main application is to explore future scenarios for large-scale integration of renewable energy. PowerGAMA uses linear programming to optimize the generator dispatch for all generators in the system based on marginal cost for each time-step over a given period. The power system is represented by nodes, branches, loads and generators, where load and generators are assigned to nodes and branches connect the nodes. The grid model is usually a reduced and simplified version of the actual grid, as explained in [11], and the actual generators and loads are aggregated and designated to the closest node. The tool is based on a simple power market configuration, assuming a perfect market where power flow constraints and generator costs determine the generator dispatch and nodal prices, minimizing the total system cost. PowerGAMA input files contain grid data and time series profiles.

In other words, the tool has the option to take into account the variability of renewable power production from hydro, solar and wind power generators, and the variability of power consumption and flexible demand. Considering energy storage, which may be implemented as individual components or integrated with certain generators, the system optimization in one time-step needs to consider the previous time-step as well. Thus, the optimal solution is found sequentially.

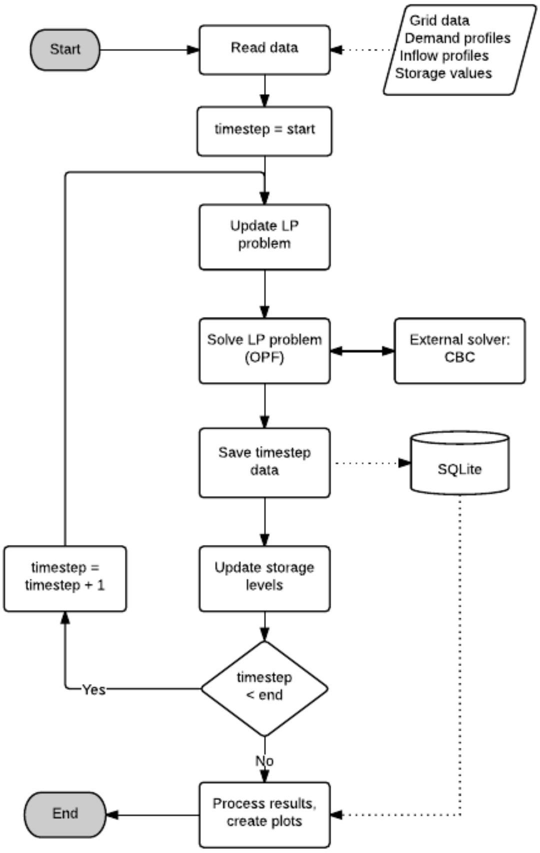
Start
Read data
Grid data
Demand profiles
Inflow profiles
Storage values
timestep = start
Update LP problem
Solve LP problem (OPF)
External solver: CBC
Save timestep data
SQLite
timestep = timestep + 1
Update storage levels
timestep < end
Yes
No
End
Process results, create plots

Figure 3.2: PowerGAMA flowchart [12]

The main algorithm implemented in PowerGAMA is outlined in the flowchart in Figure 3.2. The core of the algorithm is an optimal power flow problem (OPF) that is formulated as a standard linear programming (LP) optimization and solved for each time step. The OPF problem is linearized as explained in Section 2.2.

PowerGAMA is created with simplicity and flexibility in mind. Although it is possible to add functionality and make it more advanced, there are some clear advantages of this simplified approach. One reason is that a more complex model requires more detailed input data, which may be hard to obtain, especially when considering future scenarios. It also makes the software package more straightforward to maintain, and the results are easier to interpret and analyze when based on a simple model. Some of the simplifications include the exclusion of limits on ramp rates, start-up costs, forecast errors and barriers on utilization of power-flow on cross-border branches. Due to these simplifications the results of the analysis are considered optimistic in terms of the power system's ability to dispatch energy, and will therefore overestimate the ability to accommodate the renewable energy production. On the other hand, PowerGAMA takes the physical power flow into account, compared to models such as the EMPS model that only considers energy balance [13]. Another notable difference, in PowerGAMA the generators are modelled universally, but flexibly, with the possibility to add storage and specify the inflow for renewable energy sources.

The *IEEE Task Force on Open Source Software for Power Systems*[1] maintains a list of free, open source power tools, currently counting 21 tools. PowerGAMA is unique in its ability to perform time-series analysis with variable energy sources and energy storage. Other differences are that some of the tools require a specific program to run, which again require a license, while other lack updated input data sets. Lastly, PowerGAMA is a lightweight tool and its computational time for the presented model is approximately five hours on a regular personal computer. This enables it to be used for educational purposes and by researchers with limited resources.

An in-depth explanation of how the tool works is given in [10]. The tool can be downloaded for free from the Bitbucket web-page[2], and contributions are encouraged.

---

[1] http://ewh.ieee.org/cmte/psace/CAMS_taskforce/

[2] https://bitbucket.org/harald_g_svendsen/powergama/downloads

3.1.1 Input data structure

The input to PowerGAMA consists of CSV-files[3] that contain grid data and time series profiles. The grid data is divided into five files.

- Nodes, with names, latitudes, longitudes and country identifiers.
- Branches, between two specific nodes, with reactances and capacity limits.
- HVDC branches, between two specific nodes, with only capacity limits.
- Consumers, designated to specific nodes with average demand and demand profiles.
- Generators, designated to a specific node and assigned with a generator type, maximum production, fuel cost, reservoir level, inflow factor and an inflow profile.

Additionally, there are profiles for demand and inflow for each country. These profiles capture the hourly variation of inflow and demand throughout the year. Lastly, if storage is utilized in the model, profiles for storage filling level and time dependent factors are implemented, as explained in Section 3.1.4.

3.1.2 Model input data

The input data used to expand the existing model, and a detailed overview of changes and new sources is found in the Scenario log[4]. A brief overview is given here to accompany the mentioned files.

The raw input data is obtained from the Hutcheon and Bialek 2009 power flow model [14], which contains approximate data on nodes, branches, generation and consumption for most European countries. Data for the following countries have been obtained from [3]: Albania (AL), Austria (AT), Bosnia (BA), Belgium (BE), Bulgaria (BG), Czech Republic (CZ), Germany (DE), Denmark West (DK), Greece (GR), Croatia (HR), Hungary (HU), Luxembourg (LU), Montenegro (ME), Macedonia (MK), the Netherlands (NL), Poland (PL), Romania (RO), Serbia (RS), Slovenia (SI) and Slovakia (SK). The input data from [14] required some adjustments to be compatible with PowerGAMA, and an initial conversion was performed. The nodal coordinates from the line-diagram were exported and approximate longitudes and latitudes were calculated using inverse projections (Python script), and open branches were removed. Moreover, area names were adapted to ISO 3166 Alpha-2 codes[5] and some minor modifications were performed to ensure unique node names. Then the data was formatted to fit the PowerGAMA file format. This data set has been substantially updated to represent the status of the power system in 2014, as explained in Appendix A.

---

[3] CSV: Comma-separated values

[4] https://zenodo.org/record/54580

The other part of the input data set is taken from a 2014 Mediterranean case study [12], implemented in PowerGAMA as part of the EU funded EuroSunMed project. That study covered the countries Switzerland (CH), Spain (ES), France (FR), Italy (IT), Morocco (MA) and Portugal (PT), and is based on Hutcheon and Bialek's model [14], whereas it has been updated to 2014 values. The results from the study were compared with the actual data of 2014, and provide sufficiently accurate basis for further expansion of the data set. This data set is largely kept *as is*, and is only subject to minor modifications like the removal of duplicates.

The current data set contains 26 countries, including in total 1,539 nodes, 1,123 consumers, 1,158 generators and 2,399 branches. In addition, the model considers the exchange with neighboring countries Norway, Sweden, United Kingdom, Ukraine and Turkey. Figure 3.1 depicts all nodes and branches for the 2014 data set.

3.1.3 Modelling of energy storage

A brief explanation of storage functionality and how storage is utilized in this study is included to give the reader a better understanding of the papers.

When generators are modelled with storage, the marginal cost of generation changes. All inflow is first deposited in the storage as long as it is not full, and then the current storage value is calculated. If the storage value is lower than the calculated nodal price, the generators will produce, and if it is higher, the inflow is kept in the storage until the next time-step. The storage value is dependent on three variables; the *reference price* for the individual storage, multiplied by the *storage filling level factor* and a *time-dependent correction factor*.

The objective of the storage filling factor is to ensure that the storage is neither completely filled nor depleted. An example of the factor utilized in Paper C is illustrated in the left box of Figure 3.3. As can be seen from the figure, at 50% filling level the storage value is equal to the reference price, $\overline{\lambda}$. A reduction in the filling level increases the storage value to secure the reservoir from being emptied below acceptable levels. An increased storage filling level decreases the value, and when the filling level is very high, the value of the stored energy drops steeply to zero at full storage. This is to avoid spilling of resources.

---

[5] http://www.iso.org/iso/country_codes

The time-dependent correction factor adjusts the storage value further, and can have both a daily and seasonal component. This factor represents the knowledge of expected inflow and electricity prices, forcing the power plants to store and generate reasonably considering the expected development in the future. For thermal storage, there is no seasonal component, as thermal storages have a maximum capacity of a couple of days. Hence, it is adjusted only for the hour of the day, as illustrated in the right box in Figure 3.3. The inflow of solar occurs during the day, and naturally, the value of the stored energy declines towards the morning so that the storage is emptied when inflow is expected. Throughout the day, and towards the evening, the value increases and more energy is stored. Then, when the inflow has ended in the evening, the storage value drops and it depletes throughout the night, completing the cycle.

The seasonal component is not illustrated in the figure, but may be implemented for hydro storage plants by e.g. increasing the factor in periods with high inflow, to ensure the reservoir is filled without decreasing the storage value through the filling factor. This depends on local factors like hydrology and actual storage flexibility, e.g. in Norway, where the storage is depleted before the filling season in the spring, and filled up again for the high winter load [15].

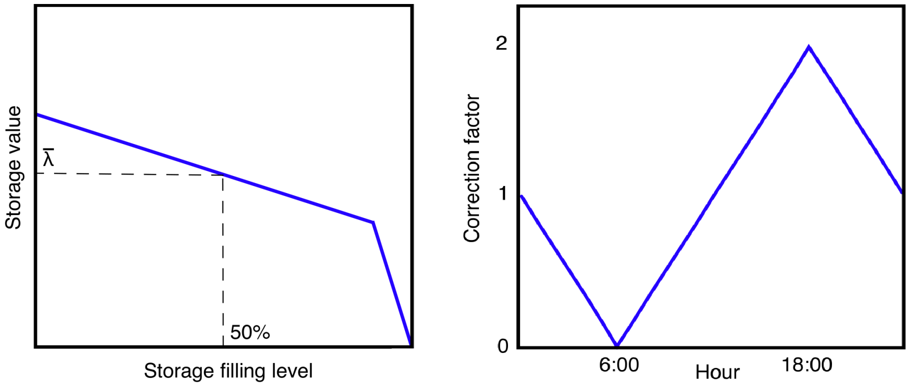

Figure 3.3: Storage value and correction factor for thermal storage

By having two correction factors depending on both filling level and time, PowerGAMA provides the opportunity to implement reasonable storage handling. Although it is not optimized, it is a simple, yet fast and powerful representation of storage systems. Additionally, PowerGAMA has the option to model storage with charging capabilities, which may represent battery technology or pumped hydro storage.

3.1.4 Modelling of pumped hydro storage

Pumped hydro storage (PHS) plants are included in the updated model, and is therefore explained in this section. For hydro plants with both generator and pump capacity, in addition to inflow, there is also an option to add energy from the power system to the storage, increasing the filling level. The dynamic of pumped hydro plants is illustrated with three different nodal prices, represented by the red points in Figure 3.4. The solid line is the storage value varying with time, while the dashed line represents a dead-band value. The dead-band value prevents continued alternations between pumping and generation over several time-steps, and indirectly considers losses due to pumping. If the nodal price is lower than the storage price and the preset dead-band value, the lowest point, the power plant pumps. If the nodal price is in the range between the storage value and the dead-band, the point in the middle, the power plant is idle. If the nodal price is higher than the storage value, the highest point, the generator produces power.

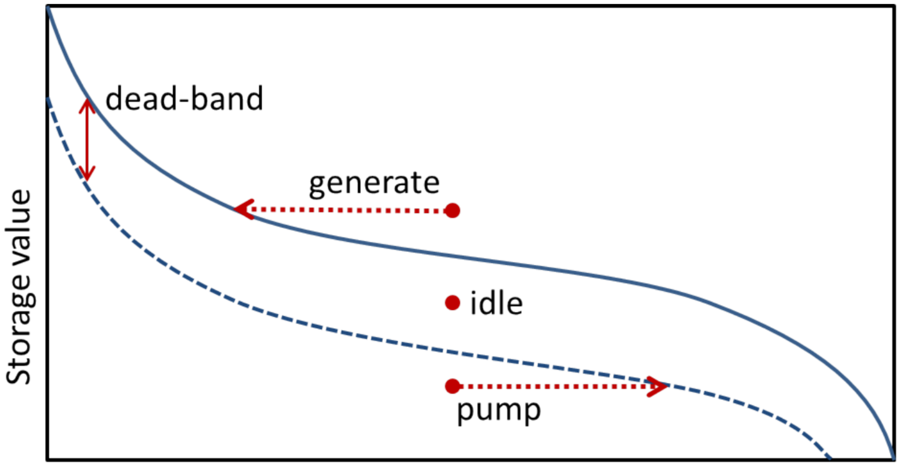

Figure 3.4: Generator with storage and pumping [10]

3.1.5 Scripts

Multiple Python scripts have been developed for this thesis, mainly to facilitate data extraction from PowerGAMA, but also to e.g. fix compatibility issues. Some of the scripts created were implemented in PowerGAMA, and are now a part of the tool's functionality. These scripts are included in appendix D.

3.1.6 Important cost functions in PowerGAMA

A parameter used in this work is the *generation cost* in a country. Subsequently, the cost of generation is the value accumulated over time in Euros (€) of generation

(MW) multiplied by fuel cost (€/MW) for each generator, plus the eventual cost of load shedding (Equation 3.1). Note that the fuel cost of generators with storage is not equal to the marginal cost, as the latter depends on the factors described in Section 3.1.3.

$$Generation\ cost = \sum_{t=1}^{T} \left[\sum_{g \in \mathcal{G}} C_g^{gen} p_{gt}^{gen} + \sum_{n \in \mathcal{N}} C^{shed} p_{nt}^{shed} \right] \tag{3.1}$$

where

$\mathcal{G}$: Set of generators

$\mathcal{N}$: Set of nodes

g : Generator

n : Node

t : Time-step

C_g^{gen} : Cost, generator g [€/MWh]

C^{shed} : Fixed cost of load shedding [€/MWh]

T : Final time-step [hour]

p_{gt}^{gen} : Generation by generator g in time-step t [MW]

p_{nt}^{shed} : Load shedding, node n, time-step t [MW]

Another important parameter is the *import cost* (€), calculated by multiplying the nodal price in the node connected to the cross-border branch (€/MWh), with the flow in the branch (MW) for each time-step:

$$Import\ cost = \sum_{t=1}^{T} \sum_{b \in \mathcal{B}} p_b \lambda_b \tag{3.2}$$

where

$\mathcal{B}$: Set of cross-border branches

b : Cross-border branch

p_b : Flow in cross-border branch b [MW]

λ_b : Nodal price, domestic node connected to branch b [€/MWh]

Positive flow represents imports and negative flow represents exports, hence the import cost will be negative when electric energy is sold.

Lastly, the *average area price* (€/MWh) is calculated as the average weighted nodal price in a country over a year:

$$Average\ area\ price = \frac{\sum_{n \in \mathcal{N}} \overline{D}_n \overline{\lambda}_n}{\overline{D}} \tag{3.3}$$

where
$\overline{D}_n$: Average consumption at node n [MWh/h]
$\overline{\lambda}_n$: Average nodal price in node n [€/MWh]
$\overline{D}$: Average total consumption in the area [MWh/h]

4 | Conclusion and Further Work

PowerGAMA has been the core of this thesis, and the work illustrates that the power simulation tool has a wide area of use. First, a model covering most of European transmission network was created before challenges regarding large-scale integration of renewable energy were investigated, and interesting results have come forth. The work is divided into three scientific papers, and the main conclusions are highlighted in this chapter.

4.1 Conclusion

The main findings from this work is grouped by the paper they were presented in.

Paper I : Validation study of an approximate 2014 European power-flow model using PowerGAMA
The paper presents a modelling approach as well as an updated and validated dataset for most of the European transmission network in 2014. By expanding the previous dataset some of the complications related to modelling the variability of RES are diminished due to cross-border flows, as peak inflow and demand varies for each country. This gives a more realistic analysis when simulating scenarios for large-scale integration of renewable energy.

Some discrepancies between aggregated actual and simulated data was observed, especially the deviation on some cross-border branches and thermal generation due to the many assumptions and simplifications implemented, as well as specific anomalies for 2014. The model responds well to modifications made to better reflect the actual conditions. The overall dynamics of the power system is adequately replicated and suitable for future analysis. The tool is especially well suited for investigating impacts of large renewable integration and storage technology, because of its ability to simulate and capture both the daily and seasonal variations.

Paper II : Analyzing large-scale renewable energy integration and energy storage in Morocco using a flow-based market model
The main challenge for the projected large-scale integration of renewable energy in Morocco is utilizing the solar generation in nodes located far from consumption centers. To facilitate the expected renewable production and demand growth, large investments in electric infrastructure is needed.

An algorithm comparing grid and storage investments based on ROI to identify investment recommendations is used. The results from the different case studies indicate that 16 branch investments can be the preferable investment strategy for Morocco, with an annual cost reduction of 279 M€, and a spillage reduction of 92 %. This case has the highest return on investment, 5.59, with almost half the investment cost of the other alternatives. On the other hand, a combination of grid and storage investments leads to the largest reduction of spillage and lowest price variations. Moreover, investment in storage reduces the need for peak reserves, but since the cost of reserves is not included in this analysis, this does not affect the ROI.

Our results indicate that grid reinforcements, or a combination of grid reinforcement and storage, could potentially accommodate a large-scale integration of renewable energy in Morocco. However, the potential for export to Europe is low due to the substantial increase in projected demand in 2030.

Paper III : The impact of large-scale renewable energy integration on the utilization of pumped hydro storage in Spain
This paper presents an approach to investigate the impact of renewable integration on pumped hydro storage (PHS) utilization. The approach is able to replicate the actual observed hydro characteristics and ensures reasonable reservoir handling.

Our results indicate that an increase in renewable generation increases the utilization of pumped hydro storage. Three scenarios are investigated, all doubling the current renewable energy output. Our results indicate that an increase in renewable generation increases the utilization of pumped hydro storage. For the scenarios with added wind and solar, and only added wind, the utilization is increased by around 150 %. The largest increase is observed in the solar scenario, at 189 %, due to a larger price reduction during solar hours.

Even though these results seem sensible regarding the utilization of PHS in Spain, no general conclusion can be drawn with respect to the impact of renewable integration on the utilization of PHS.

4.2 Further Work

During the work multiple ideas for additional analyses and model improvements were discovered.

Model improvements
Further improvements for this model could be to update the internal grid in each country, since new branches have been built in the period between 2009 and 2014.

In addition, capacity limits on internal branches could be considered.

The level of detail of the model could be increased. Implementing seasonal correction factors for hydro storage would further enhance the simulated reservoir handling and seasonal variation in hydro output, and its effect on nodal prices and the generation mix.

In many cases the availability of thermal power plants has a seasonal trend, with less available capacity during the summer. This dynamic could be modelled with inflow profiles for thermal generators.

Lastly, a more detailed classification of power plants, as well as differentiating marginal prices for each technology and area could be performed. This would for example increase the variation in nodal prices throughout the day, enabling the simulation of PHS during nighttime.

In general, these changes have the potential to further enhance the model, especially as flow-based market coupling was introduced in 2015. The validity would also be easier to assert as ENTSO-E have significantly improved the publication of data for the European power system starting in 2015.

Further analyses
Only 6-hour thermal storage with rated capacity identical to the existing CSP power plants were evaluated in Paper B. Different storage technologies and sizes, both in MW and hours, could be evaluated in further studies.

Although the work in Paper C focus on hydro storage utilization in Spain, the question is relevant, and the same methodology is applicable, for other European countries with renewable targets and existing, or ambitions for, pumped hydro storage facilities.

Other scenarios that can be investigated are, among others, new grid connections, out-phasing of nuclear power in Germany and the effects of consumer flexibility.

Bibliography

[1] International Energy Agency. (2015). World energy outlook 2015 executive summary, [Online]. Available: http://www.iea.org/publications/freepublications/publication/WEB_WorldEnergyOutlook2015ExecutiveSummaryEnglishFinal.pdf (visited on 06/01/2016).

[2] ISO New England Inc. (2013). Market operations, [Online]. Available: http://www.iso-ne.com/static-assets/documents/2014/09/m_11_market_operations_revision_47_10_06_13.doc (visited on 06/01/2016).

[3] D. Phillips. (2004). Nodal pricing basics, [Online]. Available: http://www.ieso.ca/imoweb/pubs/consult/mep/LMP_NodalBasics_2004jan14.pdf (visited on 06/01/2016).

[4] Vivi Mathiesen, NVE. (2011). Mapping of selected markets with nodal pricing or similar systems australia, new zealand and north american power markets, [Online]. Available: http://bit.ly/1HGxkFu (visited on 06/01/2016).

[5] J. J. Grainger and W. D. Stevenson, *Power System Analysis.* McGraw-Hill, 1994.

[6] D. V. Hertem, J. Verboomen, K. Purchala, R. Belmans, and W. L. Kling. (2006). Usefulness of dc power flow for active power flow analysis with flow controlling devices, [Online]. Available: http://ieeexplore.ieee.org/stamp/stamp.jsp?tp=&arnumber=1633613 (visited on 06/01/2016).

[7] Mark Jeffery, «Return on investment analysis»,

[8] M. Korpås, L. Warland, J. O. G. Tande, K. Uhlen, K. Purchala, and S. Wagemans. (2007). Tradewind d3.2:grid modelling and power system data, [Online]. Available: http://ec.europa.eu/energy/intelligent/projects/sites/iee-projects/files/projects/documents/tradewind_grid_modelling_and_power_system_data_en.pdf (visited on 06/01/2016).

[9] D. Huertas-Hernando, H. G. Svendsen, L. Warland, T. Trötscher, and M. Korpås. (2010). Analysis of off-shore grid alternatives for north sea offshore wind farms using a flow-based market model, [Online]. Available: http://ieeexplore.ieee.org/xpl/articleDetails.jsp?arnumber=5558725 (visited on 06/01/2016).

[10] H. G. Svendsen. (2015). Powergama user guide (v0.8), [Online]. Available: https://bytebucket.org/harald_g_svendsen/powergama/wiki/files/UserGuide.pdf?rev=7fa387bce1bbf184a2b088f2a4746545096f6af1 (visited on 06/01/2016).

[11] Harald G. Svendsen, «Grid model reduction for large scale renewable energy integrationanalyses», *Science direct, Jan 21, 2016*, 2015.

[12] H. G. Svendsen and O. C. Spro, «Modelling and analysis of renewable energy integration in the western mediterranean region using the powergama package», *4th Solar Integration Workshop, Berlin*, 2015.

[13] SINTEF. (2015). Efi's multi-area powermarket simulator, [Online]. Available: https://www.sintef.no/en/sintef-energy/softwareenglish/allsoftware_english/emps/ (visited on 06/01/2016).

[14] J. W. Bialek and N. Hutcheon, «Updated and validated power flow model of the main continental european transmission network», *IEEE PowerTech 2013*, 2013.

[15] O. Wolfgang, A. Haugstad, B. Mo, A. Gjelsvik, I. Wangensteen, and G. Doorman. (2009). Hydro reservoir handling in norway before and after deregulation, [Online]. Available: http://www.sciencedirect.com/science/article/pii/S0360544209003119 (visited on 06/02/2016).

A | Paper I

Title: *Validation study of an approximate 2014 European power-flow model using PowerGAMA*. Submitted to IET Generation, Transmission & Distribution 03.06.2016.

Validation study of an approximate 2014 European power-flow model using PowerGAMA

Arne Ø. Lie
Eirik A. Rye
Norwegian University of Science and Technology
Trondheim, Norway
arneovre@stud.ntnu.no, eirikary@stud.ntnu.no

Harald G. Svendsen
SINTEF Energy Research
Magnus Korpås and Hossein Farahmand
Norwegian University of Science and Technology
Trondheim, Norway

Abstract—**This paper presents a validation study of an approximated model of the European power system in 2014. A lightweight and open source power-flow tool is used for this study. The tool and model is publicly available and can be adapted to study future impact of large investments in the power system, specifically large-scale integration of renewable energy. The input data set is based on prior work, but it has been substantially updated for 2014. To maintain all aspects of the model open-source, only publicly available data was implemented. The modeling approach and simplifications are explained. Comparison of the simulation results with actual data on cross-border flows and energy mix for 2014 shows acceptable correlation, and the model is able to capture the main characteristics of the power system, i.e., reservoir handling, hydro pump pattern and seasonal variation on cross-border flows.**

Index Terms—**Energy Storage; Flow-based Market Model; Open Source; Renewable Energy Integration; Validation Study.**

I. INTRODUCTION

The power system is changing at an ever-faster rate, introducing new technology and solutions to meet the future requirements of a low emission power system. This fast developing energy transition brings new challenges for the power sector. One change is that renewable energy plants will be built in locations where the energy resources are good, often away from load centers, altering power flow patterns and likely leading to grid congestions. The transition towards more renewable energy requires many long-term investments, both in renewable generation facilities, as well as technology and infrastructure to enable the new power flow from these facilities to reach consumption centers. Due to large costs associated with infrastructure investments, long planning and construction times, and long life times, it is crucial to identify the location of future production plants and potential grid bottlenecks at an early stage. For researchers, good models with publicly available data are of key importance to study these issues.

This work addresses this by expanding a 2014 Western Mediterranean PowerGAMA data set to include most of the ENTSO-E transmission network. Since the current European power grid is one of the largest interconnected power systems in the world, it is sensible to simulate the whole system for multiple reasons. By utilizing such a large data set, some of the complications related to modelling the variability of renewable energy sources (RES) is diminished due to cross-border flows, as peak inflow and demand varies for each country. This gives a more realistic analysis when simulating scenarios for large-scale integration of renewable energy. Additionally, the model and data set can be used as a basis to analyze the effect of other major shifts in the energy sector, like the impact of large power plant investments or shut downs, e.g. the nuclear phase-out in Germany, increased hydro pump power capacity, new interconnections, or future case studies of large integration of renewable energy.

This validation study aims to give comprehensive insight into both the modelling approach and application. First, the modelling approach is explained, with the functionality of the tool, how the input data was gathered and implemented, and which modifications were necessary to tune the model. Then the major results are analyzed and their important characteristics are discussed, before concluding remarks and further work is proposed.

II. POWERGAMA PYTHON PACKAGE

The analysis is performed using the flow-based power market simulator, PowerGAMA (Power Grid and Market Analysis), developed by SINTEF Energy Research. This is a lightweight simulation tool, implemented as an open source Python package for analysis of large interconnected power systems. PowerGAMA uses linear programming to optimize the generator dispatch for all generators in the system based on marginal cost for each time-step over a given period. The power system is represented by nodes, branches, loads and generators, where load and generators are assigned to nodes, and branches connect the nodes. The grid model is usually a reduced and simplified version of the actual grid, and the actual generators and loads are aggregated and designated to the closest node. The market model assumes a perfect competition market, where power flow constraints and generator marginal costs determine the generator dispatch and nodal prices, minimizing the total system cost. The model takes into account grid constraints and variability in generation and demand using time-series input, and has the functionality to support energy storage and flexible loads.

The main algorithm implemented in PowerGAMA is outlined in the flowchart in Figure 1. The core of the algorithm is an optimal power flow problem (OPF) that is formulated as a standard linear programming (LP) optimization and solved for each time step. The OPF problem is linearized to what is commonly known as the DC power flow equations [1], only accounting for active power flow, and assuming that voltage magnitudes are equal to nominal values throughout the grid.

Considering the level of accuracy required for the high-level analysis, the approximation is considered appropriate.

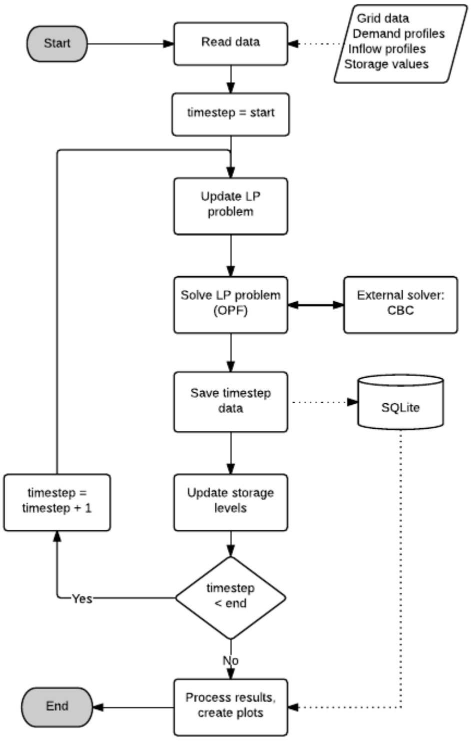
Start
Read data
Grid data
Demand profiles
Inflow profiles
Storage values
timestep = start
Update LP problem
Solve LP problem (OPF)
External solver: CBC
Save timestep data
SQLite
Update storage levels
timestep = timestep + 1
timestep < end
Yes
No
Process results, create plots
End

Figure 1. PowerGAMA flowchart [3]

A. *Mathematical formulation of PowerGAMA*

In the LP problem, the linearized power flow equations from the DC power flow method [1] are used, minimizing the system cost for each time step. The sequential approach in PowerGAMA implies a highly flexible energy market, which might be too optimistic. On the other hand, future power markets should aim to have a very high degree of flexibility to accommodate a high share of renewable energy. An advantage of a linear objective function is the short computational time, and that convergence is ensured. Fewer input parameters are also required. The linear optimization problem has the following sets, indices, parameters and variables for each time-step:

Sets

$\mathcal{G}$: Set of generators
$\mathcal{S}$: Set of pumps
$\mathcal{F}$: Set of flexible loads
$\mathcal{N}$: Set of nodes
$\mathcal{K}$: Set of AC and DC branches

Indices

g : Generator
s : Pump
f : Flexible load
n : Node
k : Branch

Parameters

C_g^{gen} : Cost, generator g [€/MWh]
C_s^{pump} : Cost, pump s [€/MWh]
C_f^{flex} : Cost, flexible load f [€/MWh]
C^{shed} : Fixed cost of load shedding [€/MWh]
P_k^{max} : Branch capacity, branch k [MW]
P_g^{min} : Minimum production, generator g [MW]
P_g^{limit} : Available power[2] generator g [MW]
$P_s^{pump,max}$: Pump capacity, pump s [MW]
$P_f^{flex,max}$: Maximum demand at flexible load f [MW]
P_n^{cons} : Consumption at node n [MW]

Variables

p_g^{gen} : Generation by generator g [MW]
p_s^{pump} : Pump power demand, pump s [MW]
p_f^{flex} : Flexible load f [MW]
p_n^{shed} : Load shedding, node n [MW]
δ_n : Power angle, node n [°]
$p_k^{ac/dc}$: Power flow, AC/DC branch k [MW]

When SC denotes the system cost of the entire system, the objective function is given as (1):

$$\min SC = \sum_{g\in\mathcal{G}} C_g^{gen} p_g^{gen} - \sum_{s\in\mathcal{S}} C_s^{pump} p_s^{pump} - \sum_{f\in\mathcal{F}} C_f^{flex} p_f^{flex} + \sum_{n\in\mathcal{N}} C^{shed} p_n^{shed}$$

Subject to (2-5):

$$-P_k^{max} \leq p_k \leq P_k^{max}, \quad k \in \mathcal{K}$$

$$P_g^{min} \leq p_g^{gen} \leq P_g^{limit}, \quad g \in \mathcal{G}$$

$$0 \leq p_s^{pump} \leq P_s^{pump,max}, \quad s \in \mathcal{S}$$

$$0 \leq p_f^{flex} \leq P_f^{flex,max}, \quad f \in \mathcal{F}$$

Where equations (2-5) are the constraints that delimit the variables. From the DC power flow equations [1], we have the power flow constraint (6):

$$\mathbf{P} = \mathbf{B'} \times \boldsymbol{\delta}$$

Where P_n is the power injection at each node, given by (7):

$$P_n = \sum_{g \in \mathcal{G}_n} p_g^{gen} - \sum_{s \in \mathcal{S}_n} p_s^{pump} - P_n^{cons} + p_n^{shed} + \sum_{k \in \mathcal{K}_n^{dc}} p_k^{dc}$$

and (8):

$$\mathbf{P_B} = (\mathbf{D} \times \mathbf{A}) \times \boldsymbol{\delta}$$

which describes the flow in the AC branches only. The last constraint is from the power flow equations is (9):

$$\delta_1 = 0$$

B. *Modelling of energy storage in PowerGAMA*

The utilization strategy of energy storage is governed by the storage value of the associated generators. If the storage value is lower than the calculated nodal price, the generators will produce, and if it is higher, the inflow is kept in the storage until the next time-step. When storage is implemented, the system optimization in one time-step needs to consider the storage level in the previous time-step as well. Thus, the optimal solution is found sequentially. The storage value is dependent on three variables; the reference price for the individual storage, multiplied by the storage filling factor and a time dependent factor. The combination of these factors enables the tool to capture the actual reservoir handling.

The objective of the storage filling factor is to ensure that the storage is neither completely filled nor depleted. The factor utilized in this study is illustrated in Figure 2. As can be seen from the figure, an increased storage filling level decreases the value to ensure resources are not spilled. A reduction in the filling level increases the storage value to secure the reservoir from being emptied below acceptable levels.

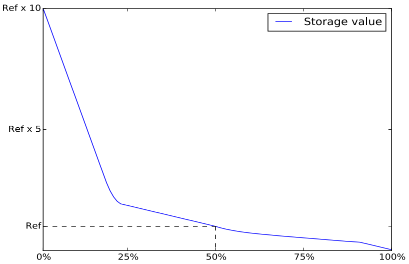

Figure 2. Storage value depending on reservoir filling level

The time dependent factor is used to capture the seasonal variations in filling level. This factor represents the knowledge of expected inflow and electricity prices, forcing the power plants to store and generate reasonably considering the expected development in the future.

By multiplying the reference price with the two factors, the model is able to replicate the actual storage filling level and reservoir handling, as can be seen in Section V. Even though this approach gives a historic reservoir handling instead of an optimal solution, it is a simple, yet fast and powerful representation of storage systems.

C. *Underlying assumptions and simplification in PowerGAMA*

Some simplifications are considered in PowerGAMA, including the exclusion of limits on ramp rates, start-up costs, forecast errors and variable barriers on utilization of cross-border branches. Due to these simplifications, the results of the analysis are considered optimistic in terms of the power system's ability to dispatch energy, and will therefore overestimate the capacity to accommodate renewable energy production. On the other hand, PowerGAMA takes the physical power flow into account, which is a significant advantage over the power market simulators that only consider energy balance, such as the EMPS[1] model. *The IEEE Task Force on Open Source Software for Power Systems*[2], maintains a list of free, open source power tools, currently counting 21 tools. PowerGAMA is unique in its ability to perform time-series analysis with variable energy sources and energy storage. Other differences are that some of the tools require a specific program to run, which again require a license, while other lack updated input data sets. Lastly, PowerGAMA is a lightweight tool and its computational time for the presented model is approximately five hours on a regular personal computer. This enables it to be used for educational purposes and by researchers with limited resources. An in-depth explanation of how PowerGAMA works is given in the PowerGAMA User Guide [2].

III. INPUT DATA

The data set is built on various publicly available sources for power data, and in this section we explain how we model and simplify certain concepts.

The European power system has an enormous amount of variables, and creating a detailed and accurate model and data set that gives the correct generation mix and flow for each hour throughout a year is beyond the scope of this study. Many simplifications have been implemented, making this an approximate data set yielding approximate simulation results. Additionally, utilities and commercial participants are often unwilling to share their data because of security reasons and commercial interests. This leads to lacking and inaccurate data, which is especially true for e.g. marginal cost of generation. However, it would be possible to create a data set that can reproduce the aggregated cross-border flow and energy production for each technology type over the course of 2014. This is possible, by e.g. adding specific limits on availability factors for every generator and cross-border branch, but it might limit some of the dynamic behavior of the power system simulation, and hence the quality of future analysis. The aim with this input data is to create a data set that represents actual data from 2014, while it is suitable for analysis of future scenarios by avoiding ad hoc restrictions that are case specific. Although this leads to simulation results that deviate from the actual data of 2014, the approach enables a more generally realistic hourly and seasonal dynamic of the different generator outputs and cross-border flows through the year, as illustrated in this paper.

The raw input data is obtained from the Hutcheon and Bialek 2009 power flow model [3], which contains approximate data on nodes, branches, generation and consumption for most European countries. Data for the following countries has been utilized directly from [3]: Austria (AT), Albania (AL), Bosnia (BA), Belgium (BE), Bulgaria (BG), Check Republic (CZ), Germany (DE), Denmark West (DK), Greece (GR), Croatia (HR), Hungary (HU), Luxembourg (LU), Montenegro (ME), Macedonia (MK), the Netherlands (NL), Poland (PL), Romania (RO), Serbia (RS), Slovenia (SI) and Slovakia (SK). The input data from [3] required some adjustments to be compatible with PowerGAMA, and an initial conversion was performed. The nodal coordinates from the line-diagram provided with the model were exported and approximate long- and latitudes were calculated via inverse projections (Python script), and open branches were removed. Moreover, area names were adapted to ISO 3166 Alpha-2 codes[3] and some minor modifications were performed to ensure unique node names. The data set has been substantially updated to represent the status of the power system in 2014, briefly explained in the following subsections.

---

[1] SINTEF, EFi's EMPS - http://www.energyplan.eu/othertools/global/emps,

[2] Task force - http://ewh.ieee.org/cmte/psace/CAMS_taskforce/software.htm

The other part of the input data set is taken from a 2014 Mediterranean case study [4], implemented in PowerGAMA as part of the EU funded EuroSunMed project [5]. That study covers the countries Switzerland (CH), Spain (ES), France (FR), Italy (IT), Morocco (MA) and Portugal (PT), and is based on Hutcheon and Bialek's model [3], whereas it has been updated to 2014 values. The results from the study were compared with the actual data of 2014, and provide sufficiently accurate basis for further expansion of the data set. This data set is largely kept *as is*, and is only subject to minor modifications like the removal of duplicates.

The current data set contains 26 countries, including in total 1,539 nodes, 1,123 consumers, 1,158 generators and 2,399 branches. In addition, the model considers the exchange with neighboring countries Norway, Sweden, United Kingdom, Ukraine and Turkey. Figure 3 depicts all nodes and branches for the 2014 data set, and the full scenario log can be studied in detail from [6].

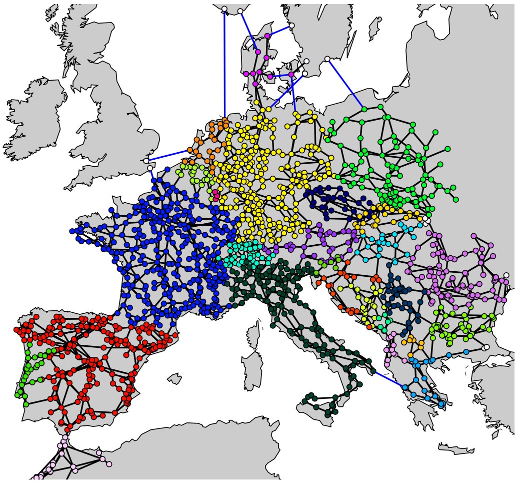

Figure 3. Location of nodes and branches for the 2014 data set

A. Nodes

Some minor changes have been performed. The geographic location of the nodes in the Benelux countries, Denmark and South Eastern Europe has been updated in accordance with the 2014 ENTSO-E Grid Map [7].

B. Branches

The input grid is taken from Hutcheon and Bialek's model of 2009 [3], where internal grids in all countries except for Morocco are modelled with unlimited branch capacity. This can be considered as a simplification that assumes the grid is adequately dimensioned. However, major changes have been made when it comes to cross-border lines. The transfer capacity on all cross-border AC lines above 220kV have been updated in accordance with [8]. Further, if data is available from [9] for the day ahead Net Transfer Capacity (NTC) values in both directions, the capacity is scaled using the mean of the highest of the bidirectional NTCs per hour in 2014. One internal AC branch in Macedonia and an HVDC branch between Denmark West and Denmark East were added, as they were missing from [3]. In addition, HVDC cables in Europe have been added using the 2014 ENTSO-E Grid Map and various sources on capacity listed in [6].

C. Consumers

The distribution of load by nodes within countries has been kept as in [3], and scaled based on 2014 annual data from ENTSO-E [8]. As [3] only contained Western Denmark, consumption for Eastern Denmark was added in accordance with [10].

D. Generators

The data sources for generators include, among several others, the 2014 ENTSO-E Grid Map, Enipedia, the Global Energy Observatory and the US DOE Global Energy Storage Database. The data set include ten generator types; coal, nuclear, gas, oil, wind, offshore wind, solar photovoltaic, concentrated solar power, hydro and other renewables. All generators were designated one of these categories, further explained in [6]. Solar and wind power generators were manually aggregated and added to nodes for all countries, and in several countries all generators were updated. In total 496 additional generators were added compared to [3] and [4]. Ultimately, the generation capacity for all countries was scaled by type based on statistical data for 2014 from ENTSO-E [8].

The marginal costs for all solar, wind and run of river hydro generators reflect the operation and maintenance cost, and were set to 0.5 €/MWh, whereas the marginal cost of hydro with storage depends on the reference price, storage filling level and time of day, and is thus variable through the year. The marginal cost for other renewables, mostly bio fuel and waste incineration, was set to 55 €/MWh, slightly below conventional power plants as described in [11], and listed in Table I. This source assumes uniform marginal costs in all countries, which is a major simplification, but an economic analysis of marginal cost for thermal plants for each country is beyond the scope of this paper. The price of load shedding is set to 1000 €/MWh.

---

[3] http://www.iso.org/iso/country_codes

TABLE I. THERMAL GENERATOR MARGINAL COST

Type	***Oil***	***Gas***	***Coal***	***Nuclear***
Marginal cost [€/MWh]	162	70	60	11

E. Storage

Information about storage size, mostly hydro reservoirs, is gathered from various sources. The exact locations of reservoirs were not obtained, and consequently reservoirs are added to all hydro plants and scaled based on each plant's rated capacity. The total reservoir for each country is given in [6]. This approach has been successfully used in [12]. Pumped hydro locations are taken from [13], and capacity from various sources as listed in [6].

F. Load, inflow and storage value profiles

The hourly load profiles for consumers and inflow profiles for renewable energy generators for each country are taken from IEE EU *TradeWind* project [12]. The storage value profiles are adapted from [4].

G. Inflow factors

The inflow factors, explained in [2], for renewable energy sources is calculated based on 2014 capacity and generation data from EuroStat [14] and ENTSO-E [8]. The availability factors for thermal power plants were implemented by setting their inflow factor equal to average annual availability in 2014 [15], [16].

H. System Boundaries

The UK, Norway, Sweden, Ukraine and Turkey are represented by one node per interconnection, with generators and/or consumers modelling the power exchange with the system boundaries. In most cases, the flow is 97-100% in one direction [8], but between Norway-Denmark and Sweden-Denmark/Germany, the flow fluctuates more frequently. These interconnections are modelled by e.g. a generator in Norway with an inflow profile equal to Norwegian exports and a consumer with a load profile equal to Norwegian imports.

IV. MODIFICATIONS OF INPUT DATA

The simulation results from the initial data set as presented above gave insufficiently accurate results, and several updates have been made to improve the correlation between the simulated results and actual observed ENTSO-E data, as explained in this Section.

A. Hydro

Numerous iterations adjusting the storage reference price for hydro power plants, storage filling factor, initial reservoir level and dead-band value for PHS (Pumped Hydro Storage) were performed in order to simulate correct hydro output.

As illustrated in Figure 4. some of the hydro inflow profiles used in the Balkan region resulted in load shedding and high nodal prices in the early spring and late winter. In order to reduce the discrepancy, these profiles were changed in accordance with [17] and [18].

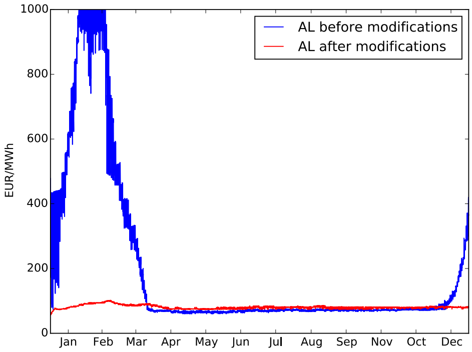

Figure 4. Nodal prices in Albania before and after modifications

B. Marginal cost

Since the preliminary input data assumes uniform marginal cost in all countries, errors concerning production and cross-border flow were expected. Marginal cost modifications in 10 countries have been implemented to reduce these discrepancies.

The most notable change was the marginal costs of thermal power in Italy and Germany. In preliminary simulations, Italy produced 25 TWh excess energy and Germany 25 TWh less energy compared to actual data, leading to increased irregular flows from south to north. As the coal mining production is significantly higher in Germany [19], and the gas price is higher in Italy [20] the marginal cost of coal and gas power plants was reduced in Germany and increased in Italy, which resulted in a more correct flow pattern.

C. Grid

Due to loop flows in the European power system [21], there is a net power flow Germany – Poland – Czech Republic – Germany. When modelling the system without capacity limits on internal branches, these flows proved hard to replicate. Since the simulated nodal prices in Germany are low and close to uniform, this leads to export to both Poland and the Czech Republic. Consequently, the same limits on internal branch capacity for Germany as used in [12] were imposed.

Using the average day ahead NTCs on cross-border branches for a year also provided some difficulties. In some cases, the average NTC is lower than the average actual flow, and on other borders, they would impede significant seasonal flow variations. In Figure 5. the actual flow from Switzerland to Italy and the average of the NTC are shown, where it highlights both issues. If line capacities were limited by NTC values, the total energy flow would be restricted by more than 4 TWh over the course of 2014.

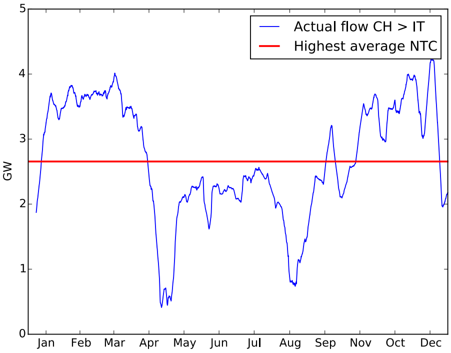

Figure 5. Actual flow (rolling weekly mean) and average NTC

D. *An example with multiple modifications*

To illustrate the improving effects of modifications, an example from simulation is presented. Albania, with 95% installed hydro capacity, experienced load shedding in the early spring and late winter. Since the load shedding price is set to 1000 €/MWh, this impacts neighboring countries by increasing exports and area prices. Additionally, flow from Central Europe was affected to support maximum flow to Albania, causing additional discrepancies.

The following sources of error were identified in Albania: the initial reservoir level was set too low, the hydro inflow profile was low in the spring and autumn while high in the summer, which is the opposite direction of actual river discharge, and the load profile did not match actual consumption. By fixing these errors, the results were significantly improved, reducing flow deviations throughout Europe and eliminating load shedding in Albania, illustrated by the average nodal prices in Figure 4.

This example highlights how sensitive the model is to coarse assumptions and minor errors, and a lot of time has been spent on investigating error sources like these.

V. RESULTS AND DISCUSSION

The results from the simulation is in this section compared to the actual recorded data from ENTSO-E [10], which is the most extensive database for European power system data. The PowerGAMA simulation tool stores results for each time step. With the input data in this study, more than 88 million variables are stored after one simulation run, and many results can be highlighted in the post processing. The emphasis in this validation study is on aggregated energy mix within a country and cross-border flow over the course of a 2014. These indicators are easy to aggregate and compare, while still giving a sufficient representation of the high-level simulation results. Additionally, time variations of energy mix, power flow and reservoir handling are highlighted.

A. *Aggregated Energy Mix*

The simulation results regarding energy mix provide sufficiently accurate results compared to actual data. TABLE II summarizes the aggregated results for each country's generation in TWh for four generation categories. Note that the category *Thermal* embraces all thermal generation including other renewables, which is mostly waste and biofuel incinerators. *Nuclear* and *Hydro* power have own categories, while *Variable RES* consists of all wind and solar technologies. The deviation between the simulated results and observed data from ENTSO-E is given as a percentage, where green implies a higher simulated generation than the reference, while negative deviations are in red.

TABLE II. ENERGY MIX (TWh)

	Thermal		***Nuclear***		***Variable RES***		***Hydro***	
AL	0.68	4%	-	-	-	-	4.1	4%
AT	13	19%	-	-	3.9	0%	45	1%
BA	9	3%	-	-	-	-	5.5	3%
BE	27	0%	32	0%	7.2	0%	1.3	3%
BG	15	25%	16	5%	2.5	0%	4.6	1%
CH	4.1	24%	26	0%	0.6	0%	40	1%
CZ	36	21%	30	3%	2.5	0%	3.1	6%
DE	350	2%	94	2%	90	0%	25	5%
DK	17	2%	-	-	13	2%	-	-
ES	100	5%	58	6%	63	1%	44	4%
FR	23	29%	420	1%	23	1%	71	4%
GR	31	2%	-	-	6.5	0%	4.9	7%
HR	2.5	16%	-	-	0.7	0%	8.1	1%
HU	8.1	22%	15	0%	0.6	0%	0.2	0%
IT	180	5%	-	-	38	0%	59	1%
LU	1.2	13%	-	-	0.1	0%	1.2	11%
MA	24	0%	-	-	2	5%	1.6	0%
ME	1.5	16%	-	-	-	-	1.7	1%
MK	5.5	49%	-	-	-	-	1.1	2%
NL	86	0%	3.9	4%	5.8	0%	-	-
PL	140	2%	-	-	7.2	0%	2.8	4%
PT	20	0%	-	-	12	2%	16	1%
RO	22	6%	11	0%	7.7	0%	19	0%
RS	28	10%	-	-	-	-	12	0%
SI	5.6	60%	6	0%	0.2	0%	6.1	2%
SK	4.6	20%	15	6%	0.4	0%	4.5	1%
Total	1154	2%	730	2%	288	0%	384	2%

Deviations between the simulation results and the ENTSO-E reference is inevitable, as the model and data set has both simplifications and approximations. In total, minor deviations concerning the total aggregated results for each category is observed. The total aggregated generation deviates 1.7 TWh from the ENTSO-E reference. The main reasons for this deviation are firstly insufficiently simulated pump power, and secondly some minor cross-border connections at the system boundary that was left out of the model.

For each country, the generation accuracy varies, but there are some general trends. The *Variable RES* generators have inflow factors based on their production time series in 2014. They have the lowest marginal costs, meaning they are dispatched first, resulting in small or no deviations aggregated over the year. *Nuclear* power plants have the second lowest marginal costs. These plants marginally overproduce when using actual availability factors. *Hydro power plants*, mostly with reservoirs, tend to overproduce. Since PowerGAMA does not support iterative water value calculations, the input modification concerning reference price and initial storage proved challenging, and did not converge towards 0 % deviation. The largest discrepancies are seen in Thermal production, which accounts for more than half of the total production. With mostly uniform prices, and no internal grid limitations, this is as expected. Overproduction of thermal energy within a country usually means that the country exports more energy than the reference, while underproduction leads to higher imports, as seen in Figure 10 and discussed in sub-section D. Another source of error is the coarse classification of the different thermal power plants, and the detailed results for these production types are not presented. Now, as all thermal generators have identical behavior in PowerGAMA, it is not deemed essential for future scenario analyzes to differentiate more on these, unless a thorough fuel cost analysis is performed.

B. Hourly generation variation

The profiles for demand and renewable generation creates a realistic hourly generation dynamic for the power system. An example of this is from June 6, with the actual (Figure 6) and June 23 simulated (Figure 7) generation mix in Germany. June 23 is chosen because it is also a Friday with high solar inflow in the simulation. Around seven AM the solar production increase rapidly in both cases, reaching a peak around midday, before declining towards the evening. Actual conventional generation is almost constant throughout the day, while simulated conventional generation varies more, possibly due to the exclusion of start-up and stop costs. Note that the production is higher in the simulated case, as more export is observed. Towards the evening, when both the demand and solar inflow decline, Germany becomes a net importer of energy in the simulated case. As can be seen, this behavior corresponds well with actual data.

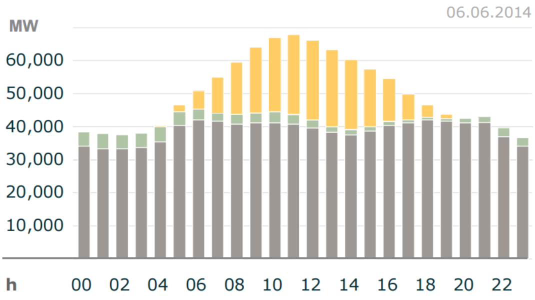

Figure 6. Actual generation mix in Germany, 06.06.2014 [22]

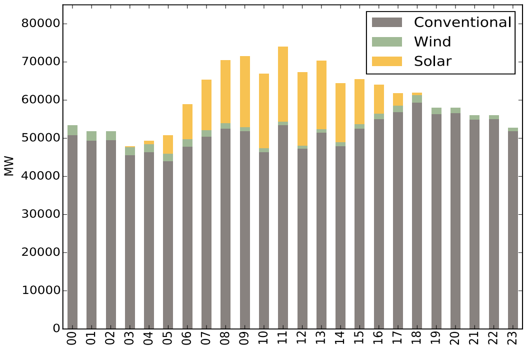

Figure 7. Simulated generation mix in Germany, 23.06.2014

C. Seasonal variation in generation

The deviation in seasonal variation of generation differs slightly from actual generation, as exemplified in Figure 8. The deviation of *Variable RES* generation was expected, as the weather in 2014 differed from the average weather that the inflow profiles are built on. Nuclear generation, on the other hand, deviates due to the assumed constant availability factor. In reality, the availability of nuclear plants is lower in summer and higher in winter, and the utilization of available capacity is close to 100% [22]. It would be possible to do an analysis on the discrepancy over several years, and create an inflow profile for nuclear that represents the availability factor over the year.

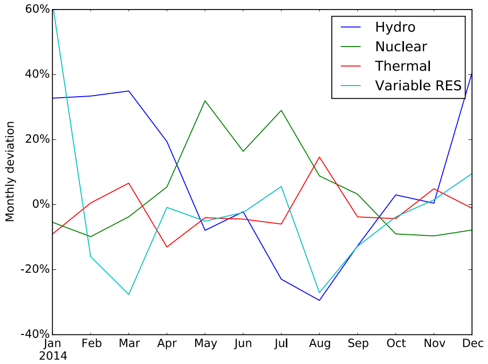

Figure 8. Monthly deviation of generation, Germany

D. Aggregated cross-border flow

The aggregated flows are illustrated in Figure 10. The direction of the arrow illustrates the direction of the actual net flow in 2014, the size of the arrow represents the magnitude of the actual flow, while the colors indicate the absolute deviation from actual net flow.

The simulated cross-border flow behaves reasonably well in Southwestern, Western and Eastern Europe. Most of these interconnections see a high share of flow going in one direction, but also interconnections with a more balanced exchange, like Spain and Portugal, see a net deviation under 20%.

The area with the highest deviating net flow is the area surrounding Austria and Slovenia. This is mainly due to the outdated grid input from 2009, causing alternated flow patterns due to grid congestions and high nodal prices in certain areas within countries. Another reason is the high marginal cost of thermal power in Greece, which was increased to facilitate exports from Italy to Greece, and to reflect the fact that the generation cost in Greece is high [23]. This enhances the southward flow, which is also generally seen in southeastern Europe.

The imposed limits on internal branches in Germany contributed to an increased flow to the Netherlands, while the net flow Germany – Poland – Czech Republic – Germany still proved difficult to reproduce. However, the flow from Germany to the Czech Republic shows the same seasonal variations as the actual flow, but is too high in the summer. This emphasizes the importance of investigating how the flow behaves over the year, as illustrated in the following sub-sections.

E. Seasonal variation on cross-border flow

One of the strengths of the PowerGAMA simulation tool is its ability to simulate the variability of renewable energy, and thus replicate some of the seasonal variation in the flow patterns, e.g. from areas with large hydropower production. There are many examples of this in the simulation results, and to illustrate this, flow between some countries that are dominated by hydropower production are highlighted. The rolling weekly mean of actual and simulated flow from Austria (AT) to Germany (DE) and from Switzerland (CH) to Germany (DE) can be studied in Figure 9**.** and Figure 11.

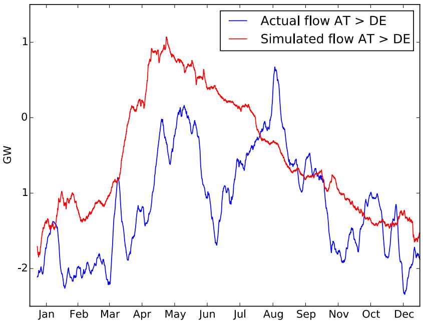

Figure 9. Actual and simulated flow from AT to DE

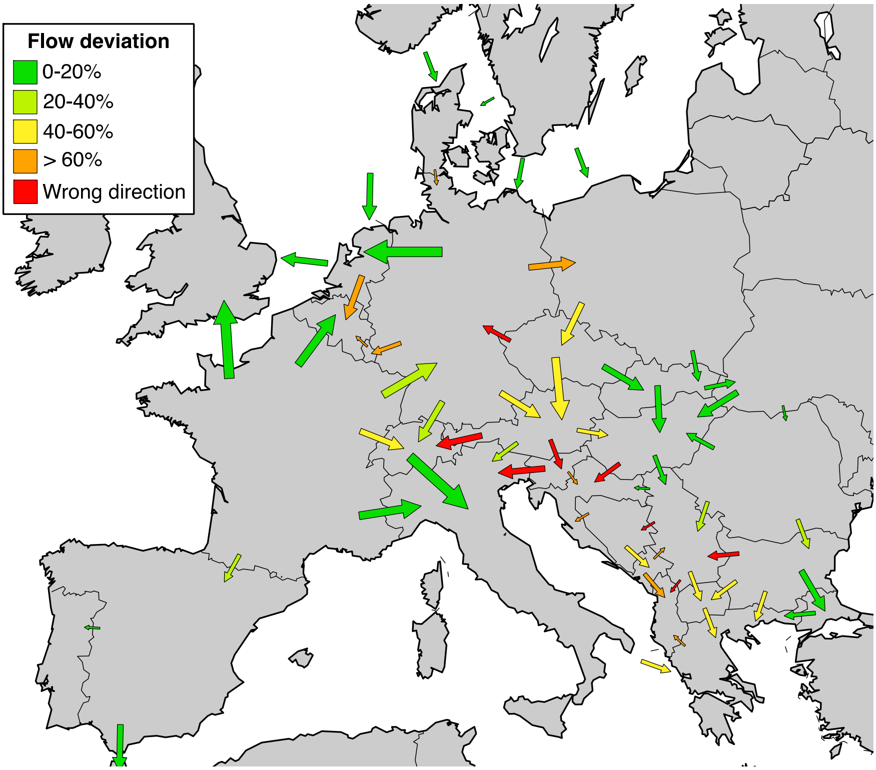

Figure 10. Cross-border flow in Europe

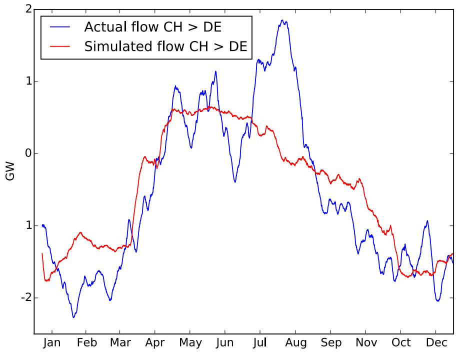

Figure 11. Actual and simulated flow from CH to DE

As seen in the figures, even though there is a deviation between the actual and simulated cross-border flow, they follow the same seasonal trend, and the model is able to replicate this dynamic. The hydro inflow during winter is lower than average in both Austria and Switzerland, leading to import of cheaper energy from Germany. When the hydro inflow increases towards the summer, the flow reverses, and especially Switzerland exports energy to Germany. Towards the winter, the inflow reduces and the flow reverses yet again. Note that the drop in actual imports to Germany between June and August is an anomaly for 2014, and is not present for 2013 or 2015. Specific anomalies for 2014 in general is a source of error for the aggregated comparison, however they should not undermine the validity of the model.

F. Seasonal hydro characteristics

To illustrate another strength of the PowerGAMA simulation tool with this data set, hydro production, reservoir handling and pumped storage dynamics are highlighted.

Generators with storage, hydro reservoirs in this case, will produce energy if the storage value is lower than the nodal price, or store energy if the storage value is higher. The storage price depends on three factors, as explained in Section II.B. With this storage representation, the actual storage strategy of hydro producers can be replicated in detail. An example of this is from Spain in Figure 12 and 13, where the factors were adjusted to capture the actual variations.

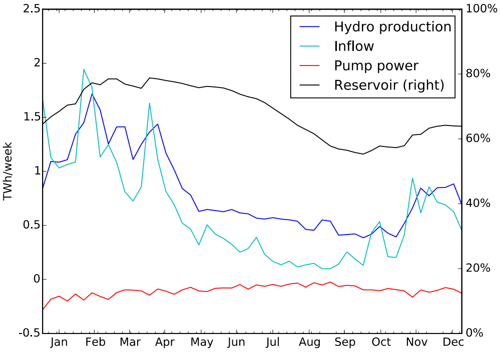

Figure 12. Actual hydro characteristics for Spain

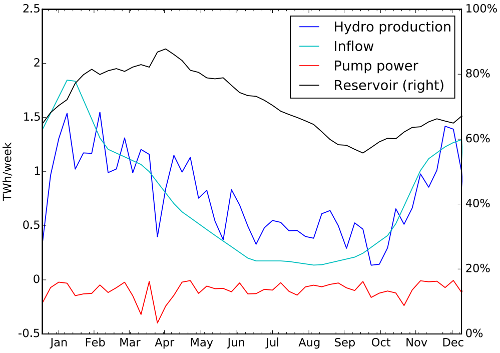

Figure 13. Simulated hydro characteristics for Spain

The inflow pattern in both cases follow the same trend, leading the annual hydro production to correlate well with actual data. The storage level is around 80 % from February until May in both cases, dropping through the summer and increasing towards the winter, ending at around 65 %.

For this study, only the seasonal correction factor for Spain was modified in order to illustrate that the model can capture the actual seasonal dynamic. For other countries, the factor has been not been implemented. In countries where the hydro reservoirs are actively managed, e.g. Austria, where it is almost completely emptied before the filling season, the storage filling level correlation between simulated and actual data is thus poor, due to the lacking seasonal factor. Further work on this part of the data set is to manually modify the seasonal correction factor for each country to improve reservoir handling.

For pumped hydro storage (PHS) plants, in addition to inflow, there is also an option to add energy from the power system to the storage, increasing the filling level. This happens if the nodal price is lower than the storage price and a preset dead-band value. The dead-band value prevents continued alternations between pumping and generation over several time-steps, and indirectly considers losses due to pumping. By manually modifying the dead-band value for PHS plants in all countries, the total pumping power simulated was 40.1 TWh, only one percent lower compared to actual data. The aggregated pump production per country also shows good precision. Note that the simulated pump production is more volatile than the actual data.

VI. CONCLUSION

This paper presents an updated and validated PowerGAMA data set for most of the European transmission network in 2014.

Some discrepancies between aggregated actual and simulated data is observed, especially the deviation on some cross-border exchanges and thermal generation due to the many assumptions and simplifications implemented, as well as specific anomalies in 2014. The model responds well to modifications made to replicate the actual conditions.

The overall dynamics of the power system are reproduced well and the model is suitable for future analysis. The tool is especially well suited for investigating impacts of large renewable integration and storage technology, because of its ability to simulate and capture both the daily and seasonal variations.

Both the tool[4] and data set[5] are available in the public domain. They can be widely used by researchers and students who want to investigate future impacts of large investments in the European power system.

VII. FURTHER WORK

In further work, we will investigate how increased solar and wind production capacity will affect the utilization of pumped hydro plants.

Even though the results of this study are sufficiently accurate for further analyses, many improvements can be implemented for more precise results, and to increase the level of detail of the model.

A more detailed classification of power plants, as well as differentiating marginal prices for each technology and area can be performed. Moreover, the availability of thermal power plants in many cases have a seasonal trend, with less available capacity during the summer. This dynamic could be modelled with inflow profiles for thermal generators.

Furthermore, implementing seasonal correction factors for hydro storage would further enhance the simulated reservoir handling and seasonal variation in hydro output, and its effect on nodal prices and the generation mix.

Updating the internal grid in each country can improve the model, since new branches have been built in the period between 2009 and 2014. In addition, capacity limits on internal branches in each country can improve the cross-border flow behavior.

In general, these changes have the potential to further enhance the model, especially as flow-based market coupling was introduced in 2015. The validity would also be easier to assert as ENTSO-E have significantly improved the publication of data for the European power system starting in 2015.

ACKNOWLEDGMENT

Parts of the research leading to these results has received funding from the European Union Seventh Framework Programme (FP7/2007-2013) under grant agreement no. 608593 (EuroSunMed).

REFERENCES

[1] J. J. Grainger and W. D. Stevenson, “Power System Analysis”. McGraw-Hill, 1994.

[2] Harald G. Svendsen, “PowerGAMA user guide”, 2015. [Online]. Available: https://goo.gl/aOViJC

[3] Neil Hutcheon and Janusz W. Bialek “Updated and validated power flow model of the main continental European transmission network” 2013. Available: http://ieeexplore.ieee.org/xpls/icp.jsp?arnumber=6652178

[4] H. G. Svendsen and O. C. Spro, “Modelling and analysis of renewable energy integration in the western mediterranean region using the powergama package” 2014, 4th Solar Integration Workshop, Berlin.

[5] EU Project, “Eurosunmed,” grant agreement no. 608593.

[6] Data set and scenario log. https://zenodo.org/record/54580

[7] ENTSO-E, «Grid map» [Online]. Available: https://goo.gl/2NqMFq

[8] ENTSO-E, “Yearly Statistics & Adequacy Retrospect” [Online]. Available: https://goo.gl/nd8b12

[9] ENTSO-E, “Transparecy platform” [Online]. Available: https://transparency.entsoe.eu/

[10] Energistyrelsen, “Energistatistikk 2014” [Online]. Available: http://goo.gl/UsRvUV

[11] Jan De Decker and Paul Kreutzkamp, “"Offshore Electricity Grid Infrastructure in Europe" 2011. [Online] Available: http://goo.gl/HL0yI2

[12] M. Korpås et al., “TradeWind D3.2:Grid modelling and power system data” 2007. [Online]. Available: http://goo.gl/esJ5by

[13] Office of Electricity Delivery & Energy Reliability, “Global Energy Storage Database” 2016. [Online]. Available: http://goo.gl/akEtOf

[14] EuroStat, “Environment and energy” [Online]. Available: http://ec.europa.eu/eurostat/data/database

[15] IAEA, ”Energy Availability Factor”. [Online]. Available: https://goo.gl/FSB58v

[16] Rick Tidball, Joel Bluestein, Nick Rodriguez and Stu Knoke, “Cost and Performance Assumptions for Modeling Electricity Generation Technologies” 2010. [Online]. Available: http://goo.gl/Fq0FfB

[17] The World bank group, “Climate change knowledge portal”, [Online]. Available: http://goo.gl/OG4PCc

[18] Agim Selencia, “Water resources of Albania”. [Online]. Available: http://medhycos.mpl.ird.fr/en/project/who/pres/alb-pre.htm

[19] KNOEMA, “International Energy Statistics” [Online]. Available: http://goo.gl/6UOy9f

[20] European Commission, “Quarterly Report on European Gas Markets.” [Online]. Available: https://goo.gl/jnj75f

[21] Thema, “Loop flows – Final advice”. 2013. [Online]. Avaiable: https://goo.gl/zPjMsd

[22] Fraunhofer institute, “Electricity production from solar and wind in Germany in 2014.” [Online]. Available: https://goo.gl/IMVYHV

[23] Greek reporter, “Why electricity in Greece is so expensive” [Online]. Available: http://goo.gl/M9ZBHe

---

[4] https://bitbucket.org/harald_g_svendsen/powergama/wiki/Home

[5] https://zenodo.org/record/54580

B | Paper II

Title: *Analyzing large-scale renewable energy integration and energy storage in Morocco using a flow-based market model.* Presented at EEM 2016, the 13th European Energy Market Conference, Faculty of Engineering of University of Porto, FEUP, from 6 to 9 of June 2016. To be published in IEEE Xplore.

Analyzing large-scale renewable energy integration and energy storage in Morocco using a flow-based market model

Eirik A. Rye
Arne Ø. Lie
Norwegian University of Science and Technology
Trondheim, Norway
eirikary@stud.ntnu.no, arneovre@stud.ntnu.no

Harald G. Svendsen
SINTEF Energy Research
Magnus Korpås and Hossein Farahmand
Norwegian University of Science and Technology
Trondheim, Norway

***Abstract*—The main objective of this paper is to investigate a 2030 scenario for the Moroccan power system and identify challenges that need to be addressed in order to integrate renewable energy and realize the potential for export. Particular emphasis is put on a cost-benefit analysis comparing investments in storage capabilities and grid reinforcements. Our results indicate that large investments in electric infrastructure is needed to accommodate the renewable commitment, and that 16 branch investments can be the preferable investment strategy for Morocco, with an annual cost reduction of 279 M€, and spillage reduction of 92 %. Storage capabilities reduce the dependency of peak reserves, but since this cost is not included in the analysis, it does not affect the profitability of storage. No export of energy to Europe is observed in any of the scenarios.**

***Index Terms*—Energy Storage; Flow-based Market Model; Investment analysis; Renewable Energy Integration.**

I. INTRODUCTION

Global warming is one of the greatest challenges of this century. The energy sector plays a vital role in the transition towards a sustainable future, and a paradigm shift in the energy sector is expected. One change is that renewable energy plants will be built in locations where the energy resources are good, often away from load centers, altering power flow patterns and likely leading to grid congestions. The transition towards more renewable energy requires many long-term investments, both in renewable generation facilities, as well as technology and infrastructure to enable the new power flow from these facilities to reach consumption centers. Due to large costs associated with infrastructure investments, long planning and construction times, and long life times, it is crucial to identify the location of future production plants and potential grid bottlenecks at an early stage.

This work addresses this issue by simulating the projected growth in renewable capacity in the Western Mediterranean region, specifically investigating the future large-scale integration of renewable energy in the Moroccan grid. Morocco possesses significant solar and wind energy resources, but today 95.6% of Morocco's total energy consumption is covered by import [1]. The Moroccan government wishes to reduce the dependency on imported energy to reduce costs and ensure energy security. Their official target is 52% installed renewable energy capacity by 2030 [2]**.** In the long-term, the ambition is to earn revenue from the export of electric energy to Europe [3].

This case study has been done in association with the EU funded EuroSunMed project [4], where SINTEF Energy Research participates. An initial part of this project was to simulate a 2014 Mediterranean case study to verify the PowerGAMA-model with input data for 2014 [5]. The results from the simulation were compared with the actual data of 2014, and they yielded sufficiently accurate basis for further analysis. Further work proposed in this part of the EuroSunMed project is to develop a 2030 scenario with a high penetration of renewable energy sources (RES). Two case studies, [6] and [7], focusing on large-scale renewable integration in Morocco have been performed using PowerGAMA. However, neither considered investment cost, hence the focus of this paper is to investigate the impact of investment costs on the integration of large scale RES in Morocco.

II. POWERGAMA PYTHON PACKAGE

The analysis is performed using the flow-based power market simulator, PowerGAMA (Power Grid and Market Analysis), developed by SINTEF Energy Research. This is a lightweight simulation tool, implemented as an open source Python package, for analysis of large interconnected power systems.

PowerGAMA uses linear programming to optimize the generator dispatch for all generators in the system based on marginal cost for each time-step over a given period. The market model is based on a perfect competition market, where power flow constraints and generator marginal costs determine the generator dispatch and nodal prices. The model takes into account grid constraints, energy storage, and variability in generation and demand using time-series input. The utilization of energy storage is represented by using marginal costs of the associated generators, which are the function of storage filling level and time of day. This is a simple, yet fast and powerful representation of storage systems. The storage utilization strategy is encoded in the dependency on filling level and time, and is given as input in the simulations. Energy storage may be implemented as individual components or integrated with certain generators. The system optimization in one time-step needs to consider the previous time-step as well. Thus, the optimal solution is found sequentially.

Some simplifications are considered in the tool, including the exclusion of limits on ramp rates, start-up costs, forecast errors and barriers on utilization of power-flow on inter-area branches. Due to these simplifications, the results of the analysis are considered optimistic in terms of the grid's power system to dispatch energy, and will therefore overestimate the ability to accommodate the renewable energy production. On the other hand, PowerGAMA takes the physical power flow into account, which is a significant advantage over the power market simulators that only consider energy balance, such as e.g. EMPS [8]. A more in-depth explanation of how the tool works is given in the PowerGAMA User guide [9].

III. CASE DESCRIPTION

The current PowerGAMA input data for this work is devoted to an analysis of a 2030 case study of the Western Mediterranean region with a high penetration of renewable energy generation. The data includes Portugal, Spain, France, Switzerland, Italy, Tunisia, Algeria and Morocco. The generation capacity, power demand, grid representation, inflow and storage for the countries in 2030 were taken from various resources, and the full case description is explained in detail in [7]. In 2014, the demand in Morocco was 25 141 GWh/year. For 2030, a projected growth of 326% to 82 000 GWh/year is estimated by the EU BETTER Project [10]. This is a conservative estimate, as other reports project up to 100-118 000 TWh [11], [12]. The steep increase in consumption is explained by expectations of a rapid population growth, urbanization, demographic changes, as well as an increase in consumption per capita due to increase in GDP.

Some modifications to the input-data of Morocco compared to [7] have been added as updated information has come forth, most notably the new target of 52% renewable energy capacity by 2030. The total generation capacity has been set to 23 391 MW, based on a 2.5 factor of installed capacity to average load. This factor is observed in many European power systems and is used as an approximation for total installed capacity. This gives an increase of 2 200 MW renewable capacity compared to [6] and [7]. The previous 2020 targets were based on solar, wind and hydro accounting for a share of 14% each [1]. However, with the hydro potential assumed fully utilized, the additional capacity has been distributed evenly between solar and wind only. Some new and planned generator locations have been identified by [13]-[15], and an upscaling in all locations has been performed to reach 52% renewable capacity. The marginal costs for hydro, solar and wind generator reflects the operation and maintenance cost, and is set to 0.5 €/MWh, while conventional as described in [16]. The total production capacity and marginal costs are summarized in TABLE I.

TABLE I. PRODUCTION CAPABILITIES

Morocco	**Production capabilities**					
	Oil	***Gas***	***Coal***	***Hydro***	***Solar***	***Wind***
Capacity [MW]	446	9000	1745	2000	5100	5100
Marginal cost [€/MWh]	162	70	60	0,5	0,5	0,5

The input grid is a reduced model with 843 nodes. The Moroccan part is derived from a detailed 2015 model using a method based on power transfer distribution factors (PTDF) that minimizes the difference between power flows in the reduced model and the full model [17]. The resulting Moroccan system consists of 34 nodes and 51 internal connections with line reactance and capacity limits constraining the power flow, and two interconnections to Spain (1400MW) and Algeria (800MW). Two branch upgrades where included in the data set to represent the newly built branch from Laayoune to Tiznit [18]. A previous analysis [6] has highlighted the challenges with increase in both demand and generation capabilities, and recommended that investment in infrastructure is necessary to enable the transition to renewable energy.

The investment costs for branches and storage are found by interpolating the costs described in [19] and [20]. These costs are annualized with an 8% return rate and a lifetime of 40 years for branches and 30 years for storage [21]. Furthermore, the costs are converted to 2007 equivalents, the same as the marginal costs of the generators. Since the actual year of investment is not decided and the investment cost of storage is expected to drop significantly in the coming years, both 2015 and 2030 investment values are considered. Operation cost of grid and storage is neglected in this analysis. The resulting investment cost are summarized in TABLE II.

TABLE II. ANNUALIZED INVESTMENT COST

Annualized Investment Cost	***2015*** *(a)*	***2030*** *(b)*
6-hour Storage [€/MW]	97 100	55 487
Grid [€/MW×km]	89.3	80.2

IV. METHOD

The goal of this study is to minimize the total cost of electricity for the Moroccan power system. The investment strategy utilized is based on ROI, (return on investment):

$$\text{ROI} = \frac{\text{Gain from investment} - \text{Cost of investment}}{\text{Cost of investment}} \qquad (1)$$

ROI evaluates the efficiency of an investment, and can be used to compare different types of investment scenarios [22]. By running the simulation for each investment alternative, the ROI can be calculated by subtracting the cost of investment from operation cost saving obtained by the investment, and divide by the cost of investment. Once the best candidate is identified, this upgrade is added to the data set and a new identification process is performed. This process is repeated as long as the ROI is positive. To shorten the calculation time for each iteration, the modelling of power exchange is simplified in this process. This is done by replacing the interconnections to Morocco with generators at the import nodes with a marginal cost equal to average nodal price. After all the investments are made, the new data set is run on the full model.

A. Case G: Grid Investments

In order to reduce the computation time, only the five branches with the most negative dual value are chosen in each iteration process, as these are the branches with the highest potential for reducing operation cost. The dual value of a branch calculated from the optimization process is a number that illustrate the constraints impact on the objective function. A marginal increase in the capacity of the branch gives a marginal change in the objective function, in magnitude given by the dual value. In other words, if the dual value of a branch is zero, the capacity constraint is not binding, and increasing the branch capacity does not affect the solution. However, if the dual value is nonzero, the branch capacity is a binding constraint, and by increasing the branch capacity, the generation cost is decreased by the magnitude of the dual value. For the nominated branches, the length is calculated by GPS-coordinates and the capacity is doubled while the reactance is halved, which is equivalent to building a new, identical branch in parallel with the existing transmission line.

B. Case S: Storage Investments

Since CSP with storage capabilities is already being built in Morocco (Noor, 580MW, 8-hours), and it is cheaper than PV-panels with battery storage [23], only CSP thermal storage is evaluated in this paper. A previous study [6] suggests that 6-hour storage size is the best when considering reduction of generation cost in Morocco, and is therefore chosen for the analysis in this paper. All locations with CSP-plants of 500 MW are assumed to have an option for storage capabilities.

C. Case GS: Grid and Storage Investments

An iterative process including all the ROIs of the CSP storage capabilities and the five branches with the lowest dual value are simulated and compared. The best investment alternative is added to the data set, and the process is repeated.

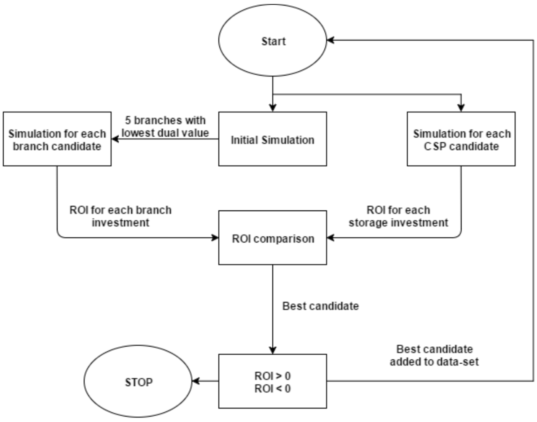
Start
5 branches with lowest dual value
Simulation for each branch candidate
Initial Simulation
Simulation for each CSP candidate
ROI for each branch investment
ROI comparison
ROI for each storage investment
Best candidate
Best candidate added to data-set
STOP
ROI > 0
ROI < 0

Ideally, all possible investments have to be simulated in all possible sequences to find the optimal investment solution, however this is not computationally feasible.

V. RESULTS AND DISCUSSION

Five different cases are analyzed. A base case (BC) without any investments, a case with only storage investments (S), a case with only grid investments (G), and lastly, two cases with a combination of storage and grid investments, for 2015 (GSa) and 2030 (GSb) investment costs.

In order to give the reader more insights to interpret the impact of grid upgrades and storage capabilities, the results of base case are presented in Figure 1. and TABLE III.

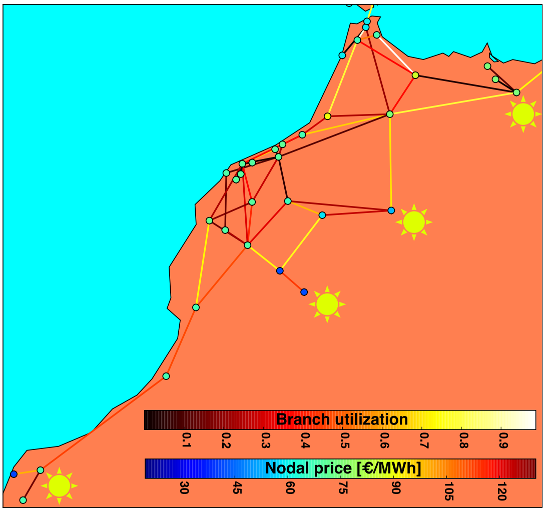

Figure 1. Location of solar power in Morocco, average branch utilization and average nodal prices in the base case.

TABLE III. BASE CASE RESULTS

	Production capabilities					
	Oil	***Gas***	***Coal***	***Hydro***	***Solar***	***Wind***
Capacity factor	6.7 %	35.7%	100%	29 %	18.9%	23.7%
Spillage [TWh]	-	-	-	0.18	3.1	0.56

The average production in Morocco is 7 749 MW, importing 547 MW from Algeria and 1 065 MW from Spain. The area price, using weighted average demand of all nodal prices, resulting in 70.59 €/MWh in Morocco, hence gas fired power plants are the price setting productions most of the time. Renewable energy share is 29.46 %, and a total spillage of 3.9 TWh is observed, meaning that as much as 14 % of the resource inflow is not utilized in the base case due to grid constraints. As spillage only occurs from renewable generators, spillage and renewable share are correlated. 80.9% of the spillage in the base case stems from solar power, mostly located far from consumption centers.

The results highlight a challenge in the Moroccan system including the discrepancy between peak solar generation and peak consumption. This could suggest that grid investments are not economically efficient. The capacity upgrades would facilitate higher flow from solar generators in hours of high renewable production and low consumption, while have a low utilization rate in off-peak hours.

TABLE IV. summarizes the results of the different case studies.

TABLE IV. COMPARISON

Results	***BC***	***Case S***	***Case G, GSa***	***Case GSb***
RES Share	29.5 %	31.8 %	33.8 %	33.8 %
Spillage	3,9 TWh	2,0 TWh	0,3 TWh	0,2 TWh
Investment Cost	-	97 M€	50 M€	92 M€
Generation cost	2,944 M€	2,823 M€	2,980 M€	2,984 M€
Import Spain	556 M€	556 M€	665 M€	665 M€
Import Algeria	372 M€	364 M€	-101 M€	-111 M€
Total Cost	3,872 M€	3,840 M€	3,593 M€	3,630 M€
Total ROI	-	0.33	5.59	2.64

A. *Investments*

The iterative process nominates two out of five thermal storage investments for Case S. 2.6 TWh solar energy resource is spilled in these two nodes in the base case scenario, which explains the investment location. The annual investment cost is 97 M€ for the storages.

In Case G, sixteen branches are selected to be expanded, of which four branches were upgraded twice. The branches from solar nodes in the south and southeast are upgraded, as well as branches towards the central consumption centers. In the north, three branches are upgraded to enable additional import from Spain. The total investment cost is 50 M€ annually.

When the grid and storage investments for 2015 (GSa) were simulated, only branch investments were decided by the investment algorithm, leading to identical results as in Case G. This is mainly due to the fact that branch upgrades reduce the profitability of storage, and as most of the grid upgrades show a higher ROI than storage, they are upgraded first. Case GSa (Grid and Stoarge 2015) is thus neglected in the following result section. It should also be noted that a single thermal storage has approximately the same investment cost as the sixteen branch investments in this case.

With investment costs for 2030 (GSb), eight branch investments are made, before one storage investment, followed by six new branches. Hence, an investment cost of 92 M€ annually is observed.

B. *Spillage and renewable share*

With increased inter-area transfer capacity or storage capabilities, the spillage is reduced, and consequently the renewable energy share increases. With two storages installed, the spillage is nearly reduced to halve, however the location and storage capacity limits further spillage reduction, resulting in 2 TWh annual spillage.

As seen from TABLE IV. with grid investments, the spillage is reduced by 92 % to 0.3 TWh. Only four of the branch upgrades are not directly or indirectly connected to nodes with solar power. Case GSb has the largest reduction of spillage by 95 %, indicating that the potential for reducing spillage is increased when combining storage and grid upgrades.

C. *Prices*

TABLE V. PRICE VARIATIONS

Area price [€/MWh]	***BC*** *(Base Case)*	***Case S*** *(Storage)*	***Case G*** *(Grid)*	***Case GSb*** *(2030 G+S)*
Average	70.59	70.29	69.33	69.46
Standard Deviation	5.55	5.40	2.94	2.34

The average annual area price is around 70 €/MWh in all cases, the same as the marginal cost of gas fired power plant. However, the standard deviation is greater with fewer upgrades, as seen in TABLE V. This is due to grid congestions that lead to spillage and higher dependence on oil fired power stations. When the transmission grid is reinforced, a higher utilization of renewable resources is possible, and the dependence on oil-fired power stations is reduced, leading to slightly lower system prices. There is also an increase in transmission between nodes, leading to fewer hours of nodal prices of 0.0 €/MWh. Subsequently, the prices are more stable. Note that the variance is even lower in Case GSb, with fewer grid upgrades and only one thermal storage. This indicates that storage can contribute more than grid upgrades to the price stability of the system.

D. *Residual load and peak load*

TABLE VI. RESIDUAL LOAD

Residual load [MW]	***BC*** *(Base case)*	***Case S*** *(Storage)*	***Case G*** *(Grid)*	***CGSb*** *(2030 G+S)*
Peak hour	12,011	11,394	12,011	11,574
Lowest hour	2,378	2,260	1,274	1,187
Capacity credit	8.90%	13.96%	8.90%	12.48%

In the base case the peak load is 13,096 MW, while the peak residual load is 12,011 MW. Based on the weather input to the case simulations, this gives a capacity credit [1] of 8.9% of total installed renewable capacity. In other words, the renewable capacity enables a 1 085 MW reduction of non-variable power production required to maintain the system adequacy. With only grid investments, the capacity credit does not change, but it increases with increasing storage capabilities. In Case GSb the capacity reduction is 1 522 MW and in Case S 1 702 MW. This indicates that storage may reduce the investments required in conventional generators, increasing the storage profitability. However, this requires a more thorough analysis based on historical weather input, which is out of scope for this paper.

E. *Generation, import and export cost*

The detailed results of each generator are not presented here, however some interesting results are highlighted. As a change in import or export affect the generation cost within Morocco, it must be considered when comparing the different cases. The import cost (€) is calculated by multiplying the nodal price (€/MWh) in the Moroccan node connected to the interconnector, with the flow (MW) over the interconnector at each time-step.

With the upgraded grid, the generation cost increases, even though the renewable share is higher than the other cases and the oil-fired power plants are completely out-priced. The reason is the increased gas production due to the notable difference in the net transfer with Algeria, turning from import in the base case to export with grid upgrades. Even though the import cost from Spain is increased by 109 M€, the total production within Morocco has increased by 501 MW.

---

[1] Capacity credits are further explained here: http://goo.gl/AmshXk

The import from Spain is limited by bottlenecks in the north, and the situation does not change when adding storage. The generation cost is reduced by 121 M€. This is mainly due to less spillage and increased RES production, which in turn displaces gas production. In the last case with grid and storage, the export to Algeria is slightly higher while the import from Spain remains constant, and thus the generation cost is higher as well.

F. Total cost and ROI

The grid investments reduce the annual cost by 279 M€, and has the highest total rate of return of 5.59. Only investing in storage reduces the annual cost by 32 M€, and is the least preferable solution. With investment values for 2030 (GSb), a combination of grid and storage reduces the cost by 242 M€, which is less profitable than only investing in grid with investment cost in 2015. Since the grid investment cost is lower in 2030, this highlights the challenges of using a single sequential investment analysis.

VI. CONCLUSION

The main challenge for the projected large-scale integration of renewable energy in Morocco is utilizing the solar generation in nodes located far from consumption centers. To facilitate the expected renewable production and demand growth, large investments in electric infrastructure is needed.

The results from the different case studies indicate that 16 branch investments can be the preferable investment strategy for Morocco, with an annual reduction of 279 M€, and spillage reduction of 92 %. This case has the highest rate of return, with almost half the investment cost of the other alternatives.

A combination of grid and storage leads to the largest reduction of spillage and lower price variations. Moreover, investment in storage reduces the need for peak reserves, however since the cost of reserves are not included in this analysis, and storage cost is high, this alternative is not the most profitable investment option.

Our results indicate that grid reinforcements or a combination of grid reinforcement and storage could potentially accommodate a large-scale integration of renewable energy in Morocco, but the potential for export to Europe is low due to the substantial increase in projected demand in 2030.

VII. FURTHER WORK

This study has illustrated how PowerGAMA may be used for analyses of future scenarios in the Western Mediterranean region. Since the European power system is strongly integrated, it would be interesting to expand the model with additional European countries. By establishing this data set, a number of other analyses can be performed.

Only 6-hour storage with rated capacity identical to the existing CSP power plant is evaluated in this paper. Different storage size, both in MW and hours, could be evaluated in further studies.

ACKNOWLEDGMENT

Parts of the research leading to these results has received funding from the European Union Seventh Framework Programme (FP7/2007-2013) under grant agreement no. 608593 (EuroSunMed).

REFERENCES

[1] World Future Council, “100% renewable energy: Boosting development in morocco,” 2015. [Online]. Available: http://goo.gl/XzQVp8

[2] The Economist, “Morocco expands its renewable energy goals,” Des. 12, 2015. [Online]. Available: http://goo.gl/QI7ZKu

[3] Bekening et al. “D 7.4: Better roadmap,“ 2015, [Online]. Available: http://goo.gl/hVruve

[4] EU Project. “Eurosunmed,” 2014, [Online]. Available: http://www.eurosunmed.eu/

[5] H. G. Svendsen et al, “Modelling and analysis of large scale solar energy integration in the Morrocan power system”, in: *4th Solar integration workshop, Berlin, Germany, Nov. 2014.*

[6] A. Ø. Lie and E. A. Rye, “Large-scale Integration of Renewable Energy in Interconnected Power Systems, Case studies of Morocco.” Unpublished, Des. 2015.

[7] H. G. Svendsen and O. C. Spro, “Modelling and analysis of renewable energy integration in the western mediterranean region using the powergama package” Submitted for publication, 2015,

[8] SINTEF, “Efi’s multi-area powermarket simulator,” [Online]. Available: http://www.energyplan.eu/othertools/global/emps/

[9] H. G. Svendsen, “Powergama user guide (v0.8),” [Online]. Available: https://goo.gl/lf9YLh

[10] F. Trieb and T. Fichter, “D3.2.1: Demand development scenarios for north africa,” 2013, [Online]. Available: http://goo.gl/5wYpsw

[11] Irena, “Case study 2013, Morocco wind atlas,” [Online]. Available: http://www.rcreee.org/sites/default/files/irena_case_morocco.pdf

[12] B. Brand. (2011), “The renewable energy targets of the Maghreb countries: Impact on electricity supply and conventional power markets,” *Energy Policy, vol 39, issue 8, August 2011, Pages 4411–4419* [Online]. Available: http://goo.gl/uyoMJz

[13] NREL, “Concentrating Solar Power Projects in Morocco,” [Online]. Available: http://goo.gl/hCrQPr

[14] AMDI, "Moroccan Investment Development Agency,” [Online], Available: http://goo.gl/kbuawr

[15] The Wind Power, “Wind Energy Market Intelligence” [Online], Available: http://goo.gl/Szq0vn

[16] H. G. Svendsen, L. Warland and M. Korpås, “OffshoreGrid D6.2: Report describing final results from the offshore power market analysis,” *Tech. rep., SINTEF Energy Research* ,2011.

[17] H. G. Svendsen, “Grid model reduction for large scale renewable energy integration analyses”, in: *12th EERA Deepwind R&D conference, Trondheim, Norway, 2015.*

[18] M. Dekkak, “New high-voltage connects Laayoune to Tiznit,” [Online] Available: http://goo.gl/qSHrf7

[19] ECN, “D3.1 Trans-national infrastructure developments on the electricity and gas market,”, p.38. 2011

[20] B. Brand, “The value of dispatchability of CSP plants in the electricity systems of Morocco and Algeria,” *Energy Policy, Vol 47, August 2012, Pages 321–331*

[21] Irena, “Concentrating Solar Power Technology Brief,” *IEA-ETSAP and IRENA© Technology Brief E10 – January 2013,* p.25.

[22] M Jeffrey, “Return on Investment Analysis,” [Online] Available: http://goo.gl/Jp6z5w

[23] M. Orosz, “Photovoltaics and concentrating solar power: Why hybridization makes sense,” [Online]. Available: http://goo.gl/6wLaiy

[24] The Guardian, “Morocco poised to become a solar superpower with launch of desert mega-project,” Oct. 25, 2015. Available: http://gu.com/p/4dh3m/sbl

C | Paper III

Title: *The impact of large-scale renewable energy integration on the utilization of pumped hydro storage in Spain.* Submitted to the 6th International Solar Integration Workshop in Vienna, 2016.

The impact of large-scale renewable energy integration on the utilization of pumped hydro storage in Spain

Eirik A. Rye
Arne Ø. Lie
Norwegian University of Science and Technology
Trondheim, Norway
eirikary@stud.ntnu.no, arneovre@stud.ntnu.no

Harald G. Svendsen
SINTEF Energy Research
Magnus Korpås and Hossein Farahmand
Norwegian University of Science and Technology
Trondheim, Norway

Abstract—**This paper investigates how a large increase in renewable generation affects the utilization of existing pumped hydro storage stations in Spain. To perform the analysis, actual data from 2014 was used, and simulations were performed with a flow-based market model. The approach is able to capture the actual hydro characteristic of the system and ensures reasonable reservoir handling in all scenarios. The results indicate that an increase in renewable generation can greatly increase the utilization of pumped hydro storage (PHS) in Spain. The utilization increases more with added solar than wind capacity, due to a larger price reduction during solar hours. Even though these results seem sensible regarding the utilization of PHS in Spain, no general conclusion can be drawn with respect to the impact of renewable integration on the utilization of PHS.**

Index Terms—**Flow-based Market Model; Open Source; Pump Hydro Storage, Renewable Energy Integration.**

I. INTRODUCTION

Political motivation and technological leaps for both wind and solar power has led to an increase of 235 GW (119%) [1] and 150 GW (300%) [2] installed capacity from 2010-2015 respectively, and the growth is expected to continue [3]. One of the largest challenges with the transition from fossil fuels to renewable energy is the large share of intermittent production from these production technologies, complicating the continuous supply of energy to the consumers' needs. One proposed solution for this challenge is investing in pumped hydro storage (PHS), which can store surplus energy when the renewable inflow is high, and produce energy when the inflow is low. 294 pumped hydro stations are currently under operation worldwide, with an aggregated capacity of 144.4 GW. These facilities represent more than 230 TWh energy storage [4], which is 98 % of the total grid connected storage capacity. Numerous studies have investigated both the technical and economic feasibility of pumped hydro plants, e.g. [5]-[8]. Many of these studies focus on the benefit PHS pose to the power system, and tries to predict the future development of PHS. This study, on the other hand, tries to shed light on how the current PHS plants utilization will be influenced by an increase in renewable generation.

Prior work [4] has established a flow-based market model of the European power system in 2014, suitable for further analysis. From this study, it is known that Spain has significant hydro resources, reservoir capacity and pump capacity, as well as installed solar and wind capacity. This study investigates how the utilization of existing PHS plants in Spain is affected by a large increase in different renewable generation technologies.

The study aims to give insight into both the modelling approach and application. First, the modelling approach is explained, with the functionality of the tool. Then the major results from the case studies are analyzed and their important features are discussed, before concluding remarks and scope for further work is proposed.

II. POWERGAMA PYTHON PACKAGE

The analysis is performed using the flow-based power market simulator, PowerGAMA (Power Grid and Market Analysis), developed by SINTEF Energy Research. This is a lightweight simulation tool, implemented as an open source Python package for analysis of large interconnected power systems. PowerGAMA uses linear programming to optimize the generator dispatch for all generator types in the system based on their marginal cost for each time-step over a given period. The market model is based on a perfect competition market, where power flow constraints and generator marginal costs determine the optimal generator dispatch and nodal prices. The model takes into account grid constraints, energy storage, and variability in generation and demand using time-series input.

A. Modelling of storage

The utilization strategy of energy storage is governed by the storage value of the associated generators. When generators are modelled with storage, the marginal cost of generation changes. All inflow is first deposited in the storage as long as it is not full, and then the current storage value is calculated. If the storage value is lower than the calculated nodal price, the generators will produce, and if it is higher, the inflow is kept in the storage until the next time-step. When storage is implemented, the system optimization in one time-step needs to consider the storage level in the previous time-step as well. Thus, the optimal solution is found sequentially. The storage value is dependent on three variables; the reference price for the individual storage, multiplied by the storage filling factor and a time dependent factor. The combination of these factors enable the tool to reproduce the actual reservoir handling.

Since the option to store or produce energy depends on the nodal price, the storage utilization can be controlled by comparing the storage value with the average nodal price. With this in mind, the reference price for hydro storage is set equal to the marginal cost of gas power, 70 €/MWh, which is the price-setting technology most of the time in this study. This is because the average load in Spain is not covered by nuclear, coal, wind and solar alone, meaning the alternative to hydro is covering the load with gas power.

The objective of the storage filling factor is to ensure that the storage is neither completely filled nor depleted. The factor utilized in this study is illustrated in Figure 1. As can be seen from the figure, an increased storage filling level decreases the value to ensure resources are not spilled. A reduction in the filling level increases the storage value to secure the reservoir from being emptied below acceptable levels. At approximately 20 % filling level the storage value is close to the load shedding cost. The slope of the curve punishes negative deviations harder when the filling level is low, and the storage value increases dramatically, while the change is more moderate in the area around e.g. 70 % filling level.

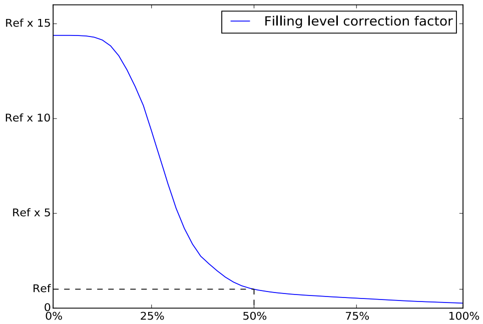

Figure 1. Storage value depending on reservoir filling level

The time dependent factor is used to capture the seasonal variations in filling level, and is shown in Figure 2. This curve represents the knowledge of expected inflow and electricity prices, forcing the power plants to store and generate reasonably considering the expected development in the future.

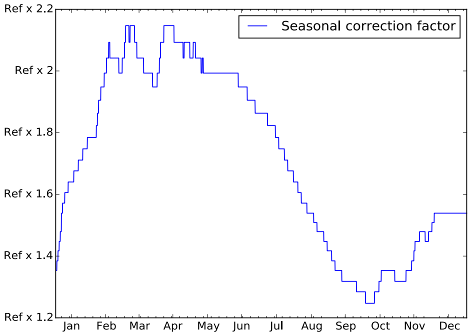

Figure 2. Storage value depending on time of year

By multiplying the reference price with the other two factors, the model is able to replicate the actual storage filling level and reservoir handling, as can be seen in Section V. The idea is that if the reservoir level in the simulation is identical to the actual reservoir level, the storage value will be approximately 70 €/MWh. Still, flexibility is ensured, as deviations in filling level will be governed by the filling correction factor. Ideally, the seasonal correction factor should be based on average reservoir filling, but in this study it is based on reservoir levels from 2014, as this data is available from previous work [4].

Even though this approach gives a historic reservoir handling instead of an optimal solution, it is a simple, yet fast and powerful representation of storage systems.

B. *Modelling of pumped hydro storage*

For hydro power plants with both generator and pump capacity, there is also an option to add energy from the power system to the storage, increasing the filling beyond inflow. The dynamic of pumped hydro plants is illustrated with three different nodal prices, represented by the red points in Figure 3. The solid line is the storage value variating with time, while the dashed line represents a dead-band value. The dead-band value prevents continued alternations between pumping and generation over several time-steps, and indirectly considers losses due to pumping. If the nodal price is lower than the storage price and the preset dead-band value, the lowest red point, the power plant enters pumping mode. If the nodal price is in the range between the storage value and the dead-band, the red point in the middle, the power plant is idle. If the nodal price is higher than the storage value (highest red point), the generator produces power. The pump efficiency is set to 90 % [9].

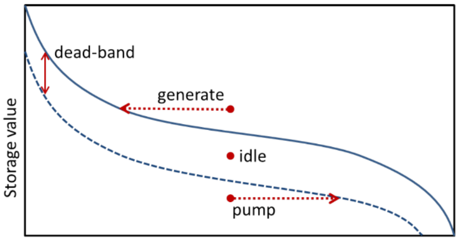

Figure 3. Generator with storage and pumping. [9]

C. *Simplifications and similar tools*

Some simplifications are considered in PowerGAMA, including the exclusion of limits on ramp rates, start-up costs, forecast errors and hourly barriers on utilization of inter-area branches. Due to these simplifications, the results of the analysis are considered optimistic in terms of the power system's ability to dispatch energy, and will therefore overestimate the capacity to accommodate renewable energy production. On the other hand, PowerGAMA takes the physical power flow into account, which is a significant advantage over the power market simulators that only consider energy balance, such as the EMPS[1] model. *The IEEE Task Force on Open Source Software for Power Systems*[2], maintain a list of free, open source power tools, currently counting 21 tools. PowerGAMA differs from many of them in functionality, with the ability to perform time-series analysis with variable energy sources and energy storage. Other differences are that some of the tools require a specific program to run, which again require a license, while others lack updated input data sets. Lastly, PowerGAMA is a lightweight tool and its computational time for the presented model is approximately five hours on a regular personal computer. This enables it to be used for educational purposes and by researchers with limited resources. An in-depth explanation of how PowerGAMA works is given in the PowerGAMA User Guide [10].

---

[1] SINTEF, EFi's EMPS - http://www.energyplan.eu/othertools/global/emps,

[2] Task force - http://ewh.ieee.org/cmte/psace/CAMS_taskforce/software.htm

III. CASE DESCRIPTION

The data set is built on various publicly available sources for power data, as explained in [4]. To shorten the calculation time for this study, only the countries around Spain (Portugal, France and Morocco) are modelled, while the exchange with their neighboring countries; Belgium, the UK, Germany, Switzerland and Italy are represented by nodes with consumption and generation equal to the cross border flow in 2014. The current data set contains four countries, including in total 581 nodes, 452 consumers, 362 generators and 980 branches. Figure 4 depict all nodes and branches for the 2014 data set.

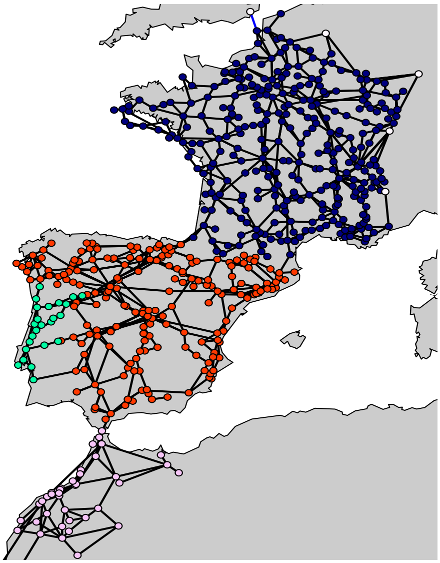

Figure 4. Location of nodes and branches for the 2014 data set

All generator capacities are taken from ENTSO-E [11]. The marginal costs for solar and wind generators reflect the operation and maintenance cost, and is set to 0.5 €/MWh, while hydro plants depend on the storage value as explained in Chapter II. Marginal cost for conventional plants are as described in [12]. The total production capacity and marginal costs for Spain are summarized in TABLE I and II.

TABLE I. CONVENTIONAL PRODUCTION CAPABILITIES IN SPAIN

Type	***Coal***	***Gas***	***Oil***	***Nuclear***	***Hydro***
Capacity [MW]	10 889	32 097	3019	7573	19 385
Marginal cost [€/MWh]	60	70	120	11	W.V

In the case study, three different scenarios are investigated. The actual output from wind and solar in Spain was 64,185 GWh in 2014, 24.9 % of total consumption. In the scenarios with increased renewable generation, the actual energy output is doubled, instead of doubling the total capacity. This is because the different technologies have different inflow factors [4], meaning one MW installed capacity of wind and solar yields different yearly output in MWh. Upscaling of installed capacity was performed at existing generator locations.

A. *Reference Scenario 2014*

The reference scenario is a simulation based on the actual data from 2014, and the results are summarized in Table II.

TABLE II. VARIABLE RES IN SPAIN – REFERENCE SCENARIO

Type	***Capacity [MW]***	***Inflow factor***	***Expected output [GWh]***
Solar CSP	2 300	0.271	5 455 (2 %)
Solar PV	4 641	0.196	7 969 (3 %)
Wind	22 846	0.255	51 028 (20 %)

For the different renewable scenarios, the expected output does not consider spillage, and the renewable energy share of total load is given as a percentage in parenthesis.

B. *Wind Scenario*

For the wind expansion scenario, the installed wind capacity is scaled so that the total renewable energy output is two times that of the reference scenario.

TABLE III. VARIABLE RES IN SPAIN – WIND SCENARIO

Type	***Capacity [MW]***	***Inflow factor***	***Expected output [GWh]***
Solar CSP	2 300	0.271	5 455 (2 %)
Solar PV	4 641	0.196	7 969 (3 %)
Wind	51 583	0.255	115 213 (45 %)

C. *Solar Scenario*

The solar scenario is scaled so that the installed capacity of CSP and PV are close to equal, while the total renewable energy output is two times that of the reference scenario. As there are more nodes with CSP than PV in the model, this avoids creating very large solar generators at certain nodes, which could lead to spilling of resources.

TABLE IV. VARIABLE RES IN SPAIN – SOLAR SCENARIO

Type	***Capacity [MW]***	***Inflow factor***	***Expected output [GWh]***
Solar CSP	18 973	0.271	45 000 (17 %)
Solar PV	18 991	0.196	32 609 (13 %)
Wind	22 846	0.255	51 028 (20 %)

D. *Diversified Renewable Scenario*

In the diversified renewable scenario, all renewable capacities are scaled so that the annual energy output for each production type is twice as much as the reference scenario.

TABLE V. VARIABLE RES IN SPAIN – DIVERSIFIED SCENARIO

Type	***Capacity [MW]***	***Inflow factor***	***Expected output [GWh]***
Solar PV	4 600	0.271	10 910 (4 %)
Solar CSP	9 282	0.196	15 938 (6 %)
Wind	45 692	0.255	102 056 (40 %)

IV. ACTUAL DATA

The actual data from Spain is presented in this chapter in order to calibrate and compare the reference scenario. The yearly hydro characteristics in Spain for 2014 is pictured in Figure 5. [10]. The inflow is highest during winter and spring, and lowest during the summer. The same is true for the hydro production. The reservoir varies between 55-80 % during 2014. Pumping is relatively stable throughout the year, but lowest during the summer.

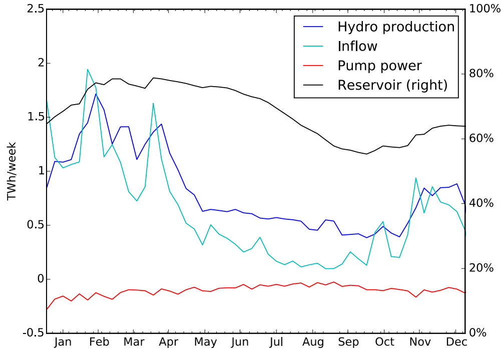

Figure 5. Actual hydro characteristics in Spain

In general, pumping occurs if the value of additional stored water is higher than the electricity price and losses. The hourly percentile graph illustrates the frequency at what time of day the pumping occurs in 2014, and is depicted in Figure 6.

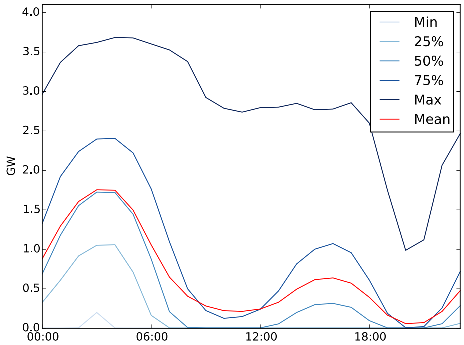

Figure 6. Hourly pumping percentiles 2014

As can be seen from the figure, the pumping usually takes place during the night when the prices are low, meaning the storage value is higher than the electricity price. From early morning until noon, the pumping is usually low, increasing slightly around midday, and very rarely is any pumping observed during the evening. This dynamic correlates well with the electricity price variation in Spain [13], as depicted in Figure 7.

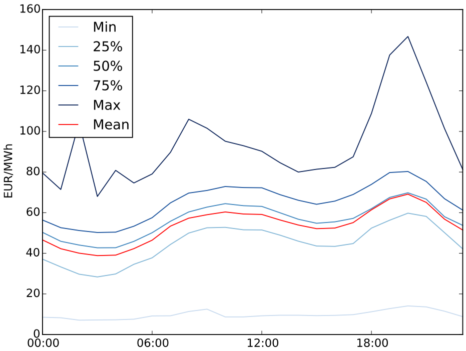

Figure 7. Hourly price percentiles 2014

V. SIMULATION RESULTS

First, the simulated reference scenario is compared with the actual data from Spain, to illustrate that the simulation is able to represent certain characteristics of the actual data. Furthermore, the different cases for renewable expansion are simulated and compared with the reference scenario. The objective is to investigate the effect of increased renewable integration on pump hydro utilization.

A. Reference scenario

The hydro characteristics in Spain observed in the reference scenario is shown in Figure 8.

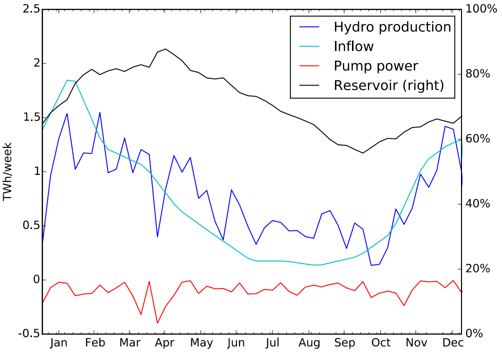

Figure 8. Simulated hydro characteristics

Compared to the actual data in Figure 5. , the overall characteristics are well replicated. Although the inflows differ, as the simulated inflow profile is based on a yearly average, the reservoir filling level and hydro production follow the same seasonal trend with a high reservoir and production in winter, and depletion of the reservoir during the summer. Less pumping is observed in the summer for both cases.

As explained in Section IV and illustrated in Figure 6. the actual pumping mainly occurs during the night in Spain. This has proven hard to replicate, as the simulated price tends to remain stable around 70 €/MWh throughout the day, with gas power as the price-setting technology. The price percentiles from the simulation is illustrated in Figure 9. The reason for this is the coarse classification of power plants in the input data, which only distinguishes between fuel types, and does not consider different power plant technologies and efficiencies. Additionally, the lack of ramp rates as well as start and stop costs for generators mean that no generators are producing when the marginal cost of production is higher than the nodal price. Consequently, the bidding curve has a lower level of detail, and simulated pumping occurs more evenly throughout the day.

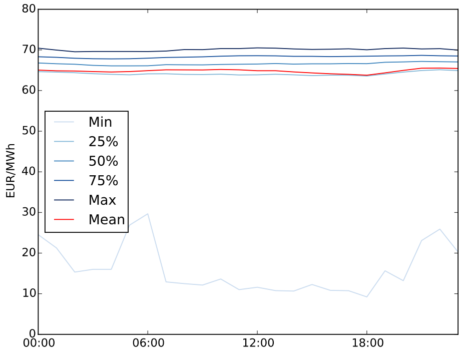

Figure 9. Hourly price percentiles, reference scenario

In Figure 10. the hourly pumping percentiles for the reference scenario is plotted. As mentioned, pumping is relatively even throughout the day, but sees a small peak around 18.00. Note that the maximum pumping power is higher in the simulated scenario. This is due to discrepancies in the input data regarding rated pump and turbine capacities, which in many cases are not differentiated even though the actual rated pumping power is lower. Additionally, there is no downtime for the simulated PHS plants.

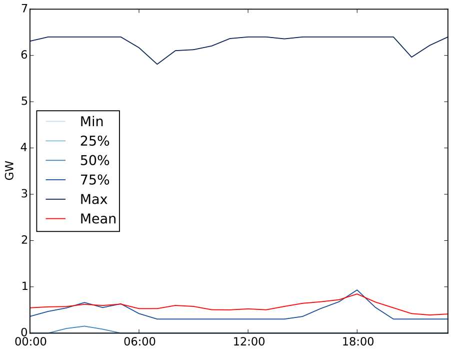

Figure 10. Hourly pump precentiles, reference scenario

Even though some discrepancies are observed, the overall dynamic is well replicated and suitable for further analysis. The aggregated actual data and results from the reference scenario are summarized on annual basis in TABLE VI.

TABLE VI. HYDRO AND PUMP COMPARISON

Type	*Hydro production [GWh]*	*Pump consumption [GWh]*
Actual	42 389	5 328
Simulated	40 596	5 001

Each renewable scenario is compared to the simulated reference case with figures, and the aggregated results are listed in tables with absolute numbers and the increase compared to the reference scenario given as a percentage in parenthesis.

B. *Wind Scenario*

TABLE VII. WIND SCENARIO - HYDRO AND PUMP

Type	*Hydro production [GWh]*	*Pump consumption [GWh]*
Simulated	45 157 (11 %)	12 250 (145 %)

The increase in wind capacity leads to more than 7 TWh additional pump energy, and a little less than 5 TWh increased hydro production. The price variation is illustrated in Figure 11. and is lower than the reference scenario on average. This leads to more pumping for every hour of the day, as well as a higher peak around 18:00, illustrated in Figure 12.

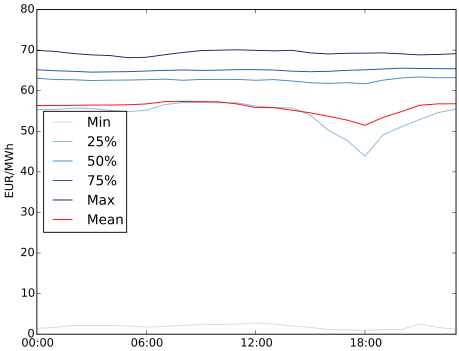

Figure 11. Hourly price percentiles, wind scenario

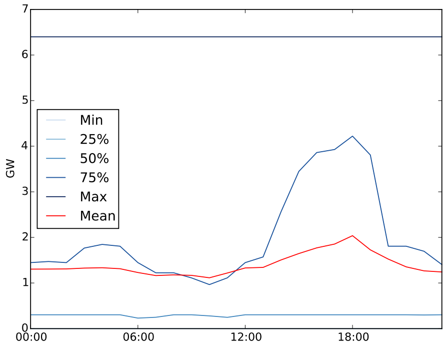

Figure 12. Hourly pump percentiles, wind scenario

C. Solar Scenario

TABLE VIII. SOLAR SCENARIO - HYDRO AND PUMP

Type	*Hydro production [GWh]*	*Pump consumption [GWh]*
Simulated	48 291 (19 %)	14 450 (189 %)

The increase in solar capacity results in close to 10 TWh more pumping than the reference scenario, and 8 TWh additional hydro production. Note that the increase in solar production reduces the price significantly during the sunshine hours compared to the other scenarios, as illustrated in Figure 13. This is seen from around 7 a.m. to 5 p.m., where the average price drops below 50 €/MWh. However, during the hours with no sun, the prices are marginally lower than the reference scenario, due to some increase in the hydro production. This results in a mid-day pumping peak that averages at 4 GW, as seen in Figure 14. In other words, the high total increase in pump power is the result of only 10 hours of lowered prices.

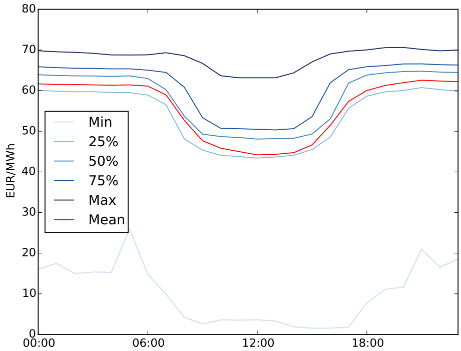

Figure 13. Hourly price percentiles, solar scenario

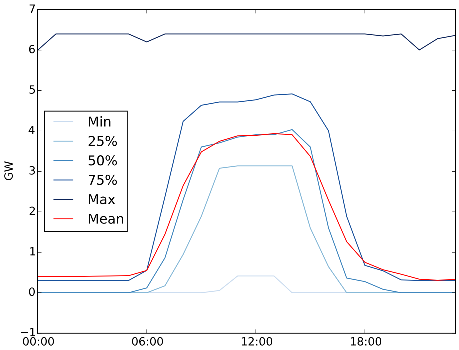

Figure 14. Hourly pump percentiles, solar scenario

D. Diversified renewable scenario

TABLE IX. DIVESRIFIED RENEWABLE SCENARIO – HYDRO AND PUMP

Type	*Hydro production [GWh]*	*Pump consumption [GWh]*
Simulated	45 196 (11 %)	12 326 (146 %)

The surge in both solar and wind capacity increases the pumping consumption by 7 TWh, and 5 TWh additional hydro production. The daily price and pump profile are similar to the wind scenario, and illustrated in Figure 15.

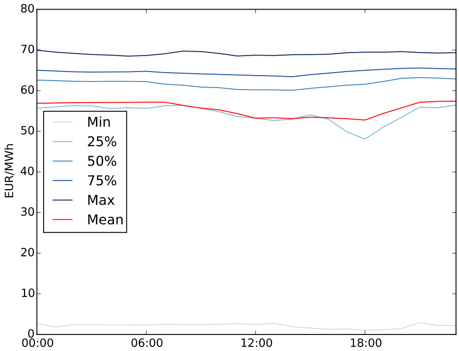

Figure 15. Hourly price percentiles, divsersified scenario

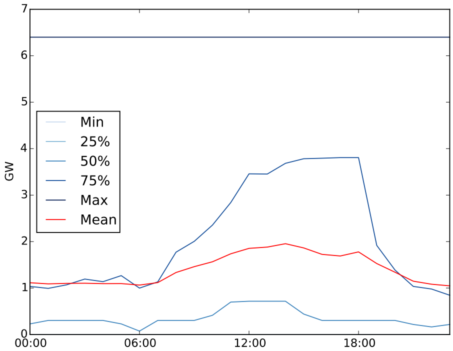

Figure 16. Hourly pump percentiles, diversified scenario

E. Reservoir handling for the different scenarios

The results of the reservoir handling for the different scenarios are illustrated in Figure 17. All the renewable scenarios show a higher filling level throughout the year, but ends at approximately the same filling level. This is due to the storage filling factor that ensures that the hydro storage does not spill energy.

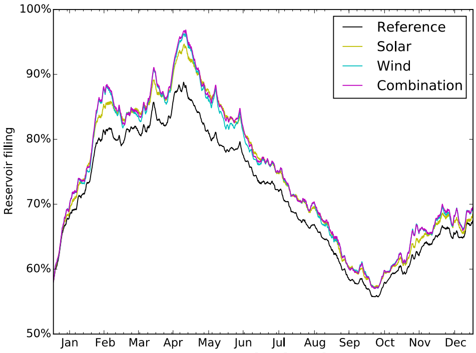

Figure 17. Reservoir levels in the scenarios

VI. DISCUSSION

The results indicate that an increase in renewable generation greatly increases the utilization of pumped hydro storage. The pumping was increased by more than 145 %, or 7 TWh, in the scenario with additional wind power and the diversified scenario, while the largest increase is observed in the solar scenario, with 189 %, or around 10 TWh additional pumping. In all cases, the increased hydro production is approximately 2 TWh lower than the increased pump energy. This is due to increased losses as the pump efficiency is 90%, and slightly higher reservoir levels at the end of the year. When pump energy varies in the scenarios, so does the final reservoir level. In general, the reservoir handling ensures sensible reservoir levels when storable energy is increased through pumping, illustrated in Figure 17.

Even though the reference scenario does not have a significant hourly price variance, the intermittent renewable generation affects both the average and hourly prices. This is especially evident for the solar scenario, Figure 13, seeing a dip in prices during daytime. If this impact was related to the actual price in Spain, Figure 7, the solar generation would possibly reduce the morning peak in prices, leading to lower price variations through the day. This effect has previously been found and described in [14].

The increase in pump power is a direct consequence of reduced nodal prices. With the simulated situation in Spain, this usually happens if gas is outpriced at the same time as the water value is high. The amount of pump power is directly related to the frequency and duration of this situation. Since solar inflow is accumulated in a shorter range of time (during daytime), it is reasonable that it influences the prices the most, leading the scenario with increased solar power to have the highest pump consumption.

It turns out that these results can represent the actual situation in Spain. Between 12:00-18:00, the prices are lower than the morning and evening peak, and pumping is more frequently observed. An increase in renewable energy further decreasing the prices in this period could lead to a high increase in pumping, as the water could be used to generate in the peak hours at a significantly higher price. The question remains to what extent this would occur, as the profitability of pump power is beyond the scope of this study.

Even though these results seem reasonable for Spain, they are not necessarily applicable for other countries, especially farther north in Europe, where the consumption and prices during daytime are higher. It is possible that an increase in solar power would shift the bidding curve, reducing the utilization of expensive power plants during the day, leading to lower peak prices and less price variations throughout the day. However, since the price is already high during daytime, this would not necessarily lead to more pumping. Total pumping might even be reduced as the profitability of pumping falls with flatter prices. On the other hand, the increased nighttime wind power production could lead to even lower prices during the night, increasing the pump utilization. The effect of renewable integration on the utilization of pumped hydro will vary from country to country for each hour over the year, depending on each countries reservoir value and bidding curves. This dynamic would have to be investigated for other countries with other system characteristics.

VII. CONCLUSION

This paper presents an approach to investigate the impact of renewable integration on pumped hydro storage utilization. The approach is able to replicate the actual observed hydro characteristics and ensures reasonable reservoir handling.

Our results indicate that an increase in renewable generation increases the utilization of pumped hydro storage. The increase when doubling the energy output of wind and wind and solar is around 146 %, while the largest increase comes from only increasing solar, at 189 %.

Even though these results can replicate the utilization of PHS in Spain, no general conclusion can be drawn with respect to the impact of renewable integration on the utilization of PHS in other countries.

VIII. FURTHER WORK

Although this work focus on hydro storage utilization in Spain, the question is relevant, and the same methodology is applicable, for other European countries with renewable targets and existing, or ambitions for, Pumped hydro storage facilities.

Additionally, a more detailed classification of power plants, as well as differentiating marginal prices for each technology could be performed to better replicate hourly price variations.

ACKNOWLEDGMENT

Parts of the research leading to these results has received funding from the European Union Seventh Framework Programme under grant agreement no. 608593 (EuroSunMed).

REFERENCES

[1] Global Wind Energy Council, “Global statistics” http://goo.gl/TyZprS

[2] Trancik et al. «Technology improvements and emissions reductions as mutually reinforcing efforts”. 2015. Available: http://goo.gl/Q8pXiU

[3] International Energy Agency, “World Energy Outlook 2013”, [Online]. Available: http://goo.gl/Tg0TJx

[4] Arne Lie and Eirik Rye, “Validation study of an approximate 2014 European power-flow model using PowerGAMA”, Work paper.

[5] LI Qiang et al. “Research on Energy Shifting Benefits of Hybrid Wind Power and Pumped Hydro Storage System Considering Peak-Valley Electricity Price”, [Online]. Available: http://goo.gl/iEA3Wj

[6] Bjarne Steffen, “Prospects for pumped-hydro storage in Germany”, 2012. [Online]. Available: http://goo.gl/uVGKmC

[7] Chi-Jen Yanga and Robert B. Jacksona, “Opportunities and barriers to pumped-hydro energy storage in the United States”, 2011. [Online]. Available: http://goo.gl/tIh55M

[8] J.P. Deane, B.P. Ó Gallachóir and E.J. McKeogh, “Techno-economic review of existing and new pumped hydro energy storage plant”, 2010. [Online]. Available: http://goo.gl/R0Zqx

[9] Ingunn Norang, “Pump Storage Hydropower for delivering Balancing Power and Ancillary Services”, Available: https://goo.gl/BlAvkt

[10] Harald G. Svendsen, “PowerGAMA user guide”, 2015. [Online]. Available: https://goo.gl/aOViJC

[11] Red Eléctrica de España, “Daily balance report” http://goo.gl/q4UtS3

[12] Jan De Decker and Paul Kreutzkamp, "Offshore Electricity Grid Infrastructure in Europe" 2011. [Online] Available: http://goo.gl/HL0yI2

[13] E·SIOS, “Statistics”, [Online]. Available: https://www.esios.ree.es/en

[14] Tveten et al. “Solar feed-in tariffs and the merit order effect: A study of the German electricity market”, 2013. Available: http://goo.gl/LZI9D3

D Scripts

The most important scripts developed for this master's thesis are presented here. The scripts for PowerGAMA were implemented in the newest release of the tool.

PowerGAMA GridData class

Class associated with all input grid data and time-dependent profiles.

```
def getDcBranches(self):
    '''
    Returns a list with DC branches in the format
    [index,from area,to area]
    '''
    hvdcBranches = []
    for idx in range(len(self.dcbranch.capacity)):
        fromNodeIdx = self.node.name.index(self.dcbranch.node_from[idx])
        toNodeIdx = self.node.name.index(self.dcbranch.node_to[idx])
        areaFrom = self.node.area[fromNodeIdx]
        areaTo = self.node.area[toNodeIdx]
        hvdcBranches.append([idx,areaFrom,areaTo])
    return hvdcBranches

def getGeneratorsWithPumpByArea(self):
    '''
    Returns dictionary with indices of generators with pumps within
    each area
    '''
    generators = {}
    for pumpIdx,cap in enumerate(self.generator.pump_cap):
        if cap>0 and cap<numpy.inf:
            nodeName = self.generator.node[pumpIdx]
            nodeIdx = self.node.name.index(nodeName)
            areaName = self.node.area[nodeIdx]
            if areaName in generators:
                generators[areaName].append(pumpIdx)
            else:
                generators[areaName] = [pumpIdx]
    return generators
```

PowerGAMA Database class

Class for storing and reading sqlite database.

```
def getResultStorageFillingArea(self,genindx,capacity,timeMaxMin):
    '''Get storage filling level for storage generators'''
    con = db.connect(self.filename)
    with con:
        cur = con.cursor()
        cur.execute("SELECT SUM(storage) FROM Res_Storage "
            +"WHERE timestep>=? AND timestep<? AND indx IN (%s)"
            % ",".join(map(str,genindx))
            +" GROUP BY timestep ORDER BY timestep",
            (timeMaxMin[0],timeMaxMin[-1]))
        rows = cur.fetchall()
        if capacity:
            values = [row[0]/capacity for row in rows]
        else:
            values = [row[0] for row in rows]
    return values

def getResultPumpPowerArea(self,genindx,negative,timeMaxMin):
    '''Get pumping for generators with pumping'''
    con = db.connect(self.filename)
    with con:
        cur = con.cursor()
        cur.execute("SELECT SUM(output) FROM Res_Pumping "
            +"WHERE timestep>=? AND timestep<? AND indx IN (%s)"
            % ",".join(map(str,genindx))
            +" GROUP BY timestep ORDER BY timestep",
            (timeMaxMin[0],timeMaxMin[-1]))
        rows = cur.fetchall()
        if negative==True:
            values = [-row[0] for row in rows]
        else:
            values = [row[0] for row in rows]
    return values
```

```
def getResultStorageValueArea(self,storageindx,timeMaxMin):
    '''
    Get average storage value (marginal price) for storage
    generators
    '''
    con = db.connect(self.filename)
    with con:
        cur = con.cursor()
        cur.execute("SELECT AVG(marginalprice) FROM Res_Storage "
            +"WHERE timestep>=? AND timestep<? AND indx IN (%s)"
            % ",".join(map(str,storageindx))
            +" GROUP BY timestep ORDER BY timestep",
            (timeMaxMin[0],timeMaxMin[-1]))
        rows = cur.fetchall()
        values = [row[0] for row in rows]
    return values
```

PowerGAMA Results class

Class for storing and analyzing/presenting results from PowerGAMA.

```
def getEnergyBalanceInArea(self,area,start_date='1/1/2014',
                  spillageGen=['hydro','solar_pv','solar_csp','wind'],
                  resolution='H',fileName='energyBalance.csv',
                  timeMaxMin=None):
    '''
    Writes time series of energy balance in an area, including
    production, spillage, load shedding, storage, pump consumption
    and imports
    '''
    if timeMaxMin == None:
        timeMaxMin = [self.timerange[0],self.timerange[-1]+1]
    prod = pd.DataFrame()
    genTypes = self.grid.getAllGeneratorTypes()
    generators = self.grid.getGeneratorsPerAreaAndType()[area]
    pumpIdx = self.grid.getGeneratorsWithPumpByArea()[area]
    storageGen = self.grid.getIdxGeneratorsWithStorage()
    areaGen = [item for sublist in list(
                        generators.values()) for item in sublist]
    matches = [x for x in areaGen if x in storageGen]

    for gt in genTypes:
        if gt in generators:
            prod[gt] = self.db.getResultGeneratorPower(generators[gt],
                                                         timeMaxMin)
            if gt in spillageGen:
                prod[gt+' spilled'] = self.db.getResultGeneratorSpilled(
                                              generators[gt],timeMaxMin)
    prod['load shedding'] = self.getLoadheddingInArea(area,timeMaxMin)
    prod['storage'] = self.db.getResultStorageFillingArea(matches,
                                                  False,timeMaxMin)
    if len(pumpIdx) > 0:
        prod['hydro pumped'] = self.db.getResultPumpPowerArea(pumpIdx,
                                                   True,timeMaxMin)
    prod['net import'] = self.getNetImport(area,timeMaxMin)
    prod.index = pd.date_range(start_date,
                            periods=timeMaxMin[-1]-timeMaxMin[0],
                            freq='H')
    if resolution != 'H':
        prod = prod.resample(resolution, how='sum')
    if fileName:
        prod.to_csv(fileName)
    else:
        return prod

def getStorageFillingInAreas(self,areas,generator_type,
                             relative_storage=True,timeMaxMin=None):
    '''
    Gets aggregated storage filling for specified area(s) for a
    specific generator type.
    '''


    if timeMaxMin == None:
        timeMaxMin = [self.timerange[0],self.timerange[-1]+1]

    storageGen = self.grid.getIdxGeneratorsWithStorage()
    storageTypes = self.grid.generator.gentype
    nodeNames = self.grid.generator.node
    nodeAreas = self.grid.node.area
    storCapacities = self.grid.generator.storage
    generators = []
    capacity = 0

    for gen in storageGen:
        area = nodeAreas[self.grid.node.name.index(nodeNames[gen])]
        if area in areas and storageTypes[gen] == generator_type:
            generators.append(gen)
            if relative_storage:
                capacity += storCapacities[gen]

        filling = self.db.getResultStorageFillingArea(generators,
                                                  capacity,timeMaxMin)

    return filling
```

Other useful scripts

Some of the other scripts made for the analyses which might be useful for others using PowerGAMA are presented here. Note that these scripts are not generalized. For the scripts used for plotting an example of output is presented.

```
'''
Plot of weekly hydro characteristics for Spain.
'''
import pandas as pd

area = 'ES'
genType = 'hydro'
timeMaxMin = [0,8760]
prodCap = 0
storCap = 0
genTypeIdx = res.grid.getGeneratorsPerAreaAndType()[area][genType]
pumpIdx = res.grid.getGeneratorsWithPumpByArea()[area]


inflowFactor = res.grid.generator.inflow_factor[genTypeIdx[0]]
# Assuming all generators have the same inflow factor
inflowProfile = res.grid.generator.inflow_profile[genTypeIdx[0]]
# Assuming all generators have the same inflow profile
for gen in genTypeIdx:
    prodCap += res.grid.generator.prodMax[gen]
    storCap += res.grid.generator.storage[gen]
output = res.db.getResultGeneratorPower(genTypeIdx,timeMaxMin)
reservoirPerc = [i*100 for i in res.db.getResultStorageFillingArea(genTypeIdx,
                                                                    storCap,timeMaxMin)]
inflow = [i*prodCap*inflowFactor for i in res.grid.inflowProfiles[inflowProfile]]
pump = res.db.getResultPumpPowerArea(pumpIdx,True,timeMaxMin)

df = pd.DataFrame()
df['Reservoir filling'] = reservoirPerc
df['Hydro production'] = output
df['Inflow'] = inflow
df['Pump power'] = pump

df.index = pd.date_range('1/1/2014',periods=timeMaxMin[-1],freq='H')
df = df.resample('7D', how={'Hydro production': 'sum', 'Pump power': 'sum',
                              'Inflow': 'sum', 'Reservoir filling': 'last'})

ax1 = df.plot(y=['Hydro production','Inflow','Pump power'],
              color=['b','c','r'],legend=False)
ax1.set_yticklabels([-0.5,0,0.5,1,1.5,2,2.5])
ax1.set_ylabel('TWh/week')
ax1.set_ylim(ymin=-500000,ymax=2500000)
ax2 =ax1.twinx()
ax2 = df['Reservoir filling'].plot(secondary_y=True,color='k')
ax2.set_xticks(['2014-01-15','2014-02-14','2014-03-16','2014-04-15',
                '2014-05-16','2014-06-15','2014-07-16','2014-08-16',
                '2014-09-15','2014-10-16','2014-11-15','2014-12-16'])
ax2.set_xticklabels(['Jan','Feb','Mar','Apr','May','Jun','Jul','Aug','Sep',
                     'Oct','Nov','Dec'])
ax2.set_yticks([0,20,40,60,80,100])
ax2.set_yticklabels(['0%','20%','40%','60%','80%','100%'])
ax2.set_ylim(ymin=0,ymax=100)
lines, labels = ax1.get_legend_handles_labels()
lines2, labels2 = ax2.get_legend_handles_labels()
labels2 = ['Reservoir (right)']
ax2.legend(lines + lines2, labels + labels2, loc=1)
ax2.set_xlim(right='2014-12-24')
```

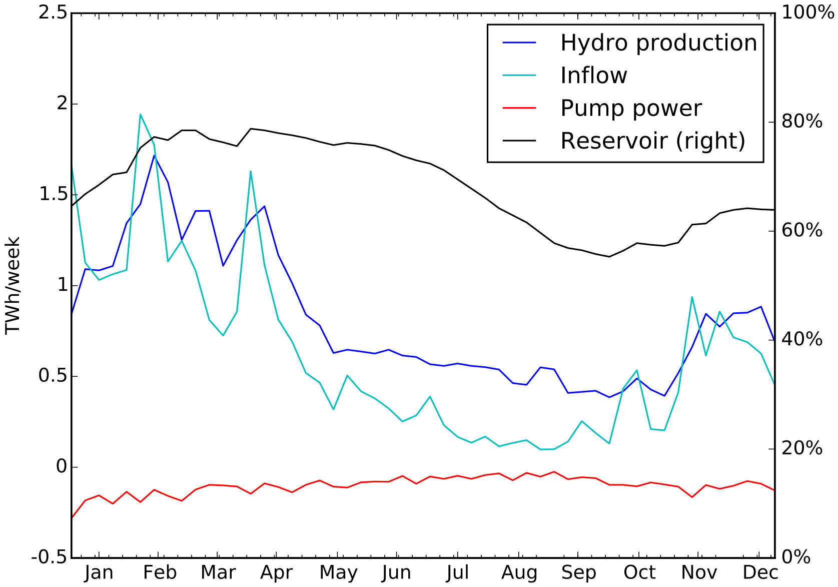

Figure D.1: Plot of weekly hydro characteristics for Spain.

```
'''
Plot of pump percentiles per hour, which may be used for prices, etc
as well.
'''
import pandas as pd

pu = pd.DataFrame()
pumpIdx = res.grid.getGeneratorsWithPumpByArea()['ES']
pu['Pump'] = res.db.getResultPumpPowerArea(pumpIdx,True,[0,8760])
#OR: pu = pu.from_csv('PumpHourly.csv',index_col=None)
pu.index = pd.date_range('1/1/2015',periods=8760,freq='H')

pu = pu*-(1/1000)

newact = pd.DataFrame()
newact['Min'] = pu['Pump'].groupby(pu.index.hour).quantile(0)
newact['25%'] = pu['Pump'].groupby(pu.index.hour).quantile(0.25)
newact['50%'] = pu['Pump'].groupby(pu.index.hour).quantile(0.5)
newact['75%'] = pu['Pump'].groupby(pu.index.hour).quantile(0.75)
newact['Max'] = pu['Pump'].groupby(pu.index.hour).quantile(1)
newact['Mean'] = pu['Pump'].groupby(pu.index.hour).mean()

ax1 = newact.plot(y=['Min','25%','50%','75%','Max'],color=['#C9DBEF',
                     '#83B7D7','#3C84BD','#154F9B','#0A2258'],legend=False)
ax1.set_xticks([0,6,12,18])
ax1.set_xticklabels(['00:00','06:00','12:00','18:00'])
ax2 = newact['Mean'].plot(color='r',legend=False)
ax2.legend(loc=1)
ax2.set_ylim(ymax=4.1)
ax2.set_ylabel('GW')
```

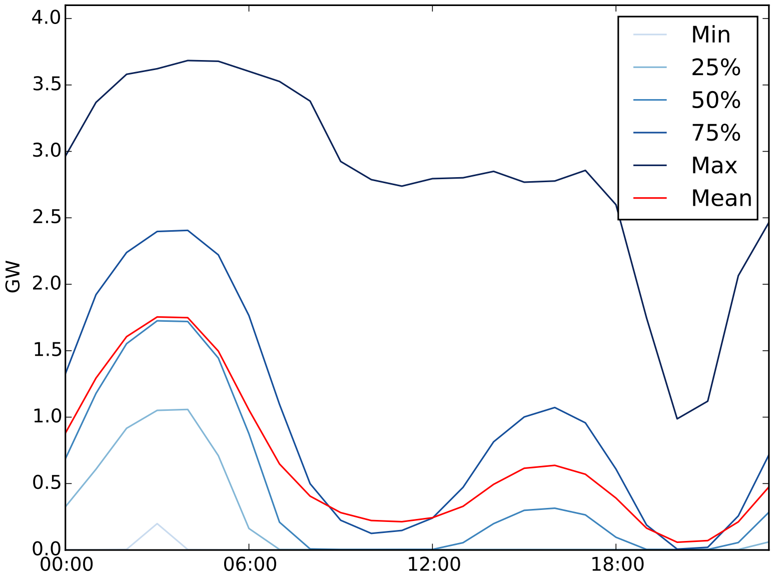

Figure D.2: Plot of pump percentiles per hour for Spain.

```
'''
Script to convert e.g. input files to utf-8 encoding
'''

import csv, ftfy

oldFile = '2014ae_ES_generators.csv'
newFile = '2014ae_ES_generators_clean.csv'
gen = []

with open(oldFile,encoding='latin1') as f:
    reader = csv.reader(f)
    for row in reader:
        genRow = []
        for i in range(len(row)):
            genRow.append(ftfy.fix_encoding(row[i]))
        gen.append(genRow)

with open(newFile, 'w', newline='', encoding='utf-8') as wf:
    writer = csv.writer(wf)
    writer.writerows(gen)

'''
Script for calculating ~length of branches in km.
'''

from geopy.distance import vincenty

f = open('Distance.txt','w')

for branch in range(53):
    nodeFromIdx = data.branch.node_fromIdx(data.node)[branch]
    nodeToIdx = data.branch.node_toIdx(data.node)[branch]
    startCoor = (data.node.lat[nodeFromIdx],
                     data.node.lon[nodeFromIdx])
    endCoor = (data.node.lat[nodeToIdx],
                     data.node.lon[nodeToIdx])
    distance = vincenty(startCoor,endCoor).km
    f.write(str(distance) + '\n')

f.close()
```

```
'''
Script returning time series of the sum of flow on interarea branches
between two areas.
'''

import csv,itertools

borderFile = 'all_borders.csv'
output = 'border_flows34.csv'
timeMaxMin = [res.timerange[0],res.timerange[-1]+1]

ac_branches = res.db.getGridInterareaBranches()
dc_branches = res.grid.getDcBranches()
border_flow = []
field_name = []

with open(borderFile) as f:
    reader = csv.reader(f)

    for border in reader:
        from_area = border[0]
        to_area = border[1]
        border_name = [from_area + '->' + to_area]
        pos_branches = []
        neg_branches = []
        ac_flow = {}
        dc_flow = {}

        for branch in ac_branches:
            if (branch[1] == from_area) and (branch[2] == to_area):
                pos_branches.append(branch[0])
            elif (branch[2] == from_area) and (branch[1] == to_area):
                neg_branches.append(branch[0])

        ac_flow = res.db.getBranchesSumFlow(pos_branches, neg_branches,
                                            timeMaxMin, acdc='ac')

        pos_branches = []
        neg_branches = []
        for branch in dc_branches:
            if (branch[1] == from_area) and (branch[2] == to_area):
                pos_branches.append(branch[0])
            elif (branch[2] == from_area) and (branch[1] == to_area):
                neg_branches.append(branch[0])

        dc_flow = res.db.getBranchesSumFlow(pos_branches, neg_branches,
                                            timeMaxMin, acdc='dc')

        border_flow.append(border_name +
                          [ac_pos + dc_pos - ac_neg - dc_neg for
                           ac_pos, ac_neg, dc_pos, dc_neg in
                           itertools.zip_longest(ac_flow['pos'],
                           ac_flow['neg'], dc_flow['pos'],
                           dc_flow['neg'],fillvalue=0)])

        print('Finished ' + from_area + '->' + to_area)

with open(output, 'w') as wf:
    writer = csv.writer(wf)
    for row in border_flow:
        writer.writerow(row)

print('CSV saved as ' + output)
```